Antiviral immune responses in lumpfish (*Cyclopterus lumpus*) – with emphasis on type I interferons

By Amanda Kästel Sandal Fond

Thesis submitted in partial fulfilment of the requirements for the degree of Master of Science

Department of Biological Sciences

Faculty of Mathematics and Natural Sciences

University of Bergen

June 2021

TAKK TIL

Arbeidet med dette prosjektet har blitt gjennomført ved Fiske Immunologi gruppen ved Institutt for Biovitenskap, Universitetet i Bergen.

Aller først vil jeg rette en stor takk til min veileder førsteamanuensis Gyri T. Haugland. Tusen takk for spennende oppgave, og ikke minst fantastisk veiledning, engasjement og hjelp underveis. Jeg er utrolig takknemlig for at din dør alltid har stått åpen og all tid du har brukt på å hjelpe meg både underveis og i sluttspurten. Uansett tid på har du alltid stilt opp, noe jeg setter veldig stor pris på. Jeg har lært veldig mye av deg som jeg vil ta med meg videre.

Videre vil jeg takke Anita Rønneseth og resten av Fiske Immunologi gruppen for et veldig godt miljø, hyggelige stunder og deres engasjement. En spesiell takk vil jeg rette til Harald S. Lunde for hjelp med alt mulig rart. Alt fra teknisk hjelp til arbeid på lab.

Tusen takk til gjengen på lesesalen for at dere har gjort mine fem år på UiB uforglemmelige. En spesiell takk til Susanne, Emina, Stian, Anna og Sara for et fantastisk siste år. Ikke minst takk overingeniør ved Institutt for Biovitenskap, Grethe Aarebakke for hyggelige avbrekk ved printeren, motivasjon og lykkeønskninger.

Tusen takk til venner, familie og gjengen på Øvre-Eide Gård for støtte og avbrekk fra lab-arbeid og skriving. Takk for at dere har prøvd å sette dere inn i oppgaven min og for alltid å holde motivasjonen min oppe. Spesiell takk til mormor og mamma som alltid har sørget for at frysen har vært full av hjemmelaget mat, det har kommet veldig godt med etter lange dager på lab.

Bergen, Juni 2021
Amanda K.S Fond

TABLE OF CONTENT

SELECTED ABBREVIATIONS

CARD	—	Caspase recruitment domain
CL	—	Cell lysate
CRFB	—	Cytokine receptor family B
HK	—	Head kidney
HKL	—	Head kidney leukocyte
IFN	—	Interferon
IFNAR	—	Interferon alpha and beta receptor
IKK	—	Inhibitor of NF-κB (IκB) kinase
IL	—	Interleukin
IRF	—	Interferon regulatory factor
ISG	—	Interferon-stimulated gene
ISGF	—	Interferon stimulated gene factor
ISRE	—	Interferon stimulated response element
JAK	—	Janus kinase
LGP2	—	The laboratory of genetics and physiology 2
LRR	—	Leucine-rich repeat
MAVS	—	Mitochondrial antiviral-signaling protein
MDA5	—	Melanoma differentiation-associated protein 5
MITA	—	Stimulator of interferon genes
Mx	—	Myxovirus resistance protein
MyD88	—	Myeloid differentiation primary response protein
NF-kB	—	Nuclear factor kappa B
NLR	—	NOD-like receptor
NOD	—	Nucleotide-binding and oligomerization domain
ON	—	Over night
PAMP	—	Pathogen-associated molecular pattern
POLYI:C	—	Polyinosinic:polycytidylic acid
PRR	—	Pattern recognition receptor
RIG-I	—	Retinoic acid-inducible gene I
RLR	—	RIG-I- like receptor
SARM	—	Sterile-alpha and Armadillo motif containing protein
SDS-PAGE	—	Sodium dodecyl sulphate-polyacrylamide gel electrophoresis
STAT	—	Signal transducer and activator of transcription proteins
TANK	—	TRAF family member associated NF-κB activator
TBK	—	TANK-binding kinase
TIRAP	—	Toll/interleukin-1 receptor domain-containing adapter protein
TLR	—	Toll-like receptor
TRAF	—	Tumor necrosis factor (TNF) receptor associated factor
TIR	—	Toll/interleukin-1 receptor
TRIF	—	TIR domain-containing adapter-inducing interferon-β
TRIM	—	Tripartite motif family
TYK	—	Tyrosine kinase

ABSTRACT

Lumpfish is an important species in the Atlantic salmon farming industry, used as biological control agent of salmon louse. As a new species produced by the aquaculture, it suffers from high mortality caused by both bacterial and viral infections, due to lack of preventive measures. However, there is currently limited knowledge about its antiviral responses and biology in general.

Upon viral infections, pattern recognition receptors (PRRs) such as RIG-like receptors (RLRs), recognize conserved pathogen motives, including viral ssRNA and dsRNA, activating signaling pathways resulting in transcription of interferons (IFNs). Type I IFNs are cytokines pivotal for first-line antiviral defense in vertebrates, through inducing transcription of interferon induced genes (ISGs) such as Mx and viperin. Once antiviral proteins are produced, the cells enter antiviral state where virus replication is inhibited.

In this study, transcriptome analysis of the RLR pathway in lumpfish was performed, revealing prescense of most components excepts RIG-I. Furthermore, three *IFN* candidates were characterized and sub-grouped through bioinformatical and phylogenetic analysis, revealing presence of IFNc, IFNd and IFNh. The basal levels of IFNs in nine healthy tissues were examined through qPCR, showing low constitutive expression in most tissues. Furthermore, gene expression analysis of *IFNs* in head kidney leukocytes (HKLs) following exposure to different PAMPs showed that *IFNc* and *IFNh*, but not *IFNd*, were highly upregulated upon exposure to polyI:C and R848 which mimic viral pathogen-associated molecular patterns (PAMPs). *IFNd* showed low, but significant upregulation following bacterial exposure. *In vivo* stimulation with polyI:C showed similar results, with high upregulation of *IFNc* and *IFNh*, in HK and spleen, but not *IFNd*, suggesting that the two formers play a role in antiviral defense in lumpfish. To confirm this, and to investigate IFNs´ ability to induce expression of ISGs, recombinant IFNc and IFNh were produced. Unfortunately, neither were soluble.

A greater understanding of antiviral immune responses in lumpfish is essential and can contribute to development of preventive measures such as vaccines protecting against viral diseases, which are needed for a sustainable farming and continuing use of lumpfish as delousing agent in the years to come.

1. INTRODUCTION

Infestation by salmon louse (*Lepeophtheirus salmonis*) is a major fish health problem for the Norwegian Atlantic salmon (*Salmo salar*) farming industry, with an estimated annual cost of USD 525 million (Jensen et al., 2020). Use of chemotherapeutant removing lice have dominated control efforts for the last four decades, leading to widespread resistance to most of the active compounds and mecanical delousing measures used raise ethical problems due to side effects (Aaen et al., 2015). Therefore, one alternative method applied is biological control of sea lice by use of cleaner fish, such as lumpfish (*Cyclopterus lumpus*) (Overton et al., 2020, Powell et al., 2018, Haugland et al., 2018). Lumpfish was first farmed in culturing facilities in Norway in 2012, where they are kept until transferred to net pens together with the salmon, where they feed on the lice.

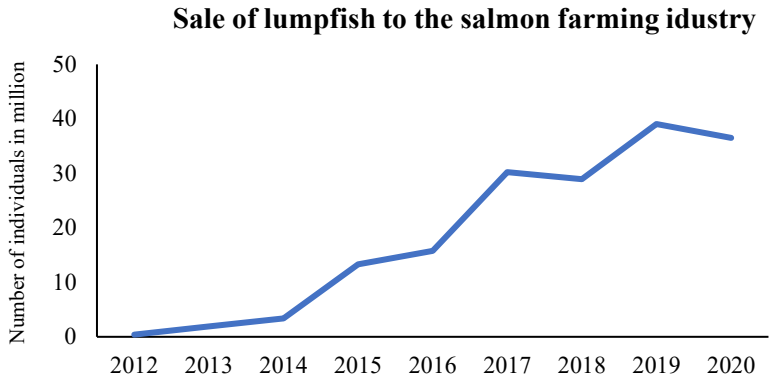

Figure 1.1 Sale of *farmed* lumpfish to the salmon farming industry from 2012-2020. Numbers are in million (source: Directorate of Fisheries, 2012).

As a newly emerging species in aquaculture, several threats to sustainable production and use of lumpfish have been identified, with diseases being one of the most prominent and potentially devastating. As culturing of lumpfish has intensified there has been a corresponding increase in the number of pathogens reported, causing bacterial and viral infections. Still the number of incidents with serious disease outbreaks are increasing. In 2015, 50% of the individuals died in the culturing facilities (Skoge et al., 2018). Screening for pathogens, revealed presence of both bacteria, parasites and viruses. The latter includes Cyclopterus Lumpus virus (CLuV) (Skoge et al., 2018) also known as lumpfish flavivirus (LFV). Additionally, Cyclopterus Lumpus Totivirus (CLuTV), Cyclopterus Lumpus Coronavirus (CLuCV), Viral hemorrhagic Septicemia Virus (VHSV), Lumpfish Ranavirus and Infections Pancreas Necrosis Virus (IPNV) have been detected, emphasizing an emerging threat to future use of lumpfish (Table 1.1) (Haugland et al., 2020).

Tabell 1.1 Overview of virus detected in lumpfish.

Virus	Disease	References
Cyclopterus lumpus virus		(Skoge et al., 2018)
Viral hemorrhagic septicemia virus (VHSV)	Viral hemorrhagic septicemia	(Scholz et al., 2018, Guethmundsdottir et al., 2019)
Lumpfish ranavirus	Ranavirosis	(Scholz et al., 2018, Stagg et al., 2020)
Infectious pancreas necrosis virus (IPNV)	Infectious pancreas necrosis	(Scholz et al., 2018, Breiland et al., 2014)
Cyclopterus lumpus totivirus (CLuTV)		(Johansen and Nylund, 2021)
Cyclopterus lumpus coronavirus (CLuCV)		(Johansen and Nylund, 2021)

1.1 The immune system of teleosts

Teleosts are continuously exposed to microbes in the water, making them more prone to microbial invasions than mammals. To prevent serious infections, the immune system needs to recognize and restrict/eliminate invading pathogens such as virus and bacteria and develop immunological memory. The immune system of vertebrates is composed of two main components: innate immune system and adaptive/acquired immune system. The innate immune system act as the first line defense against invading pathogens and includes both physical barriers as well as humoral and cellular responses. Acquired immunity is characterized by high pathogen specificity and is involved in eliminating pathogens in the initial phase of infection as well as systemic infections and provides long-term protection through immunological memory (Lazarte et al., 2019, Akira et al., 2006).

Invading pathogens are primarily blocked/limited through physical barriers such as the mucus, scales and epithelium in addition to innate humoral factors and non-specific phagocytic cells. As teleosts do not have bone marrow nor lymph nodes, their primary immune organs are head kidney (HK), spleen and thymus where immune cells are generated (Castro, 2015). Secondary lymphoid organs where antigen-presentation takes place include spleen, HK and the mucosa-associated tissues (MALTs). The MALTs comprise of skin-associated tissue (SALT), gut-associated tissue (GALT), gill associated

tissue (GiALT) and nasopharynx-associated lymphoid tissue (NALT) (Haugland et al., 2018).

If pathogens succeed in penetrating the physical barriers, other components of the immune system are triggered. The immune cells (leukocytes) involved in first line defense are present in both tissue and bloodstream, and includes monocytes, macrophages, neutrophils, dendritic cells and B cells (Castro, 2015). The main leukocytes of the adaptive immune system include B and T cells, which recognize antigens (Haugland et al., 2018, Salinas, 2015, Castro, 2015). In lumpfish, all the main types of leukocytes have been described (Haugland et al., 2012, Haugland et al., 2018), including phagocytic B cells (Rønneseth et al., 2015).

1.2 Viral recognition in teleosts

In teleosts, innate immunity is of vital importance as their adaptive immune system is considered to be less developed than in mammals (Haugland et al., 2012). In presence of invading pathogens, the innate immune system is activated through a diversified system of germline-encoded receptors termed pattern recognition receptors (PRRs) localized at the surface and/or in the cytoplasm of the host cell (Nerbøvik et al., 2017, Aoki et al., 2013). PRRs are expressed constitutively in the host and recognizes conserved pathogen motifs, termed pathogen-associated molecular patterns (PAMPs), that include proteins, lipids, lipoproteins, glycans and nucleic acids (Zou, 2016). Many fish pathogenic viruses have double- or single stranded RNA genomes. Once viruses are recognized and viral PAMPs activate PRRs, a signaling cascade is initiated leading to production of type I interferons (IFNs) and inflammatory cytokines to fight off the infection (Zou and Secombes, 2011).

1.3 Pattern recognition receptors (PRRs)

PRRs are mainly expressed in cells of the innate immune system such as dendritic cells, macrophages, monocytes and neutrophiles. Different PRRs reacts with specific PAMPs, leading to activation of specific signaling pathways and thus distinct antimicrobial responses (Akira et al., 2006, Jeannin et al., 2008). The receptors can either be soluble or cell-associated and are categorized into three groups according to their functions: soluble bridging (secreted) PRRs, endocytic PRRs and signaling PRRs. The soluble bridging PRRs mediates recognition and elimination of pathogens by phagocytes, whilst endocytic

receptors facilitate recognition and internalization of microbes and/or microbial moieties (Jeannin et al., 2008). Signaling PRRs differ in the fact that they are involved in cell-activation in response to PAMPs, ensuring that the initiated response is tailored to the invading pathogen, and are further categorized into three families; nucleotide-oligomerization domain (NOD)-like receptors (NLRs), toll-like receptors (TLRs) and retinoic acid inducible gene (RIG)-I-like receptors (RLRs) (Fig.1.2). TLRs are expressed both on the cell surface and in endosomes, whilst NLRs and RLRs primarily are localized in the cytosol (Aoki et al., 2013, Lazarte et al., 2019).

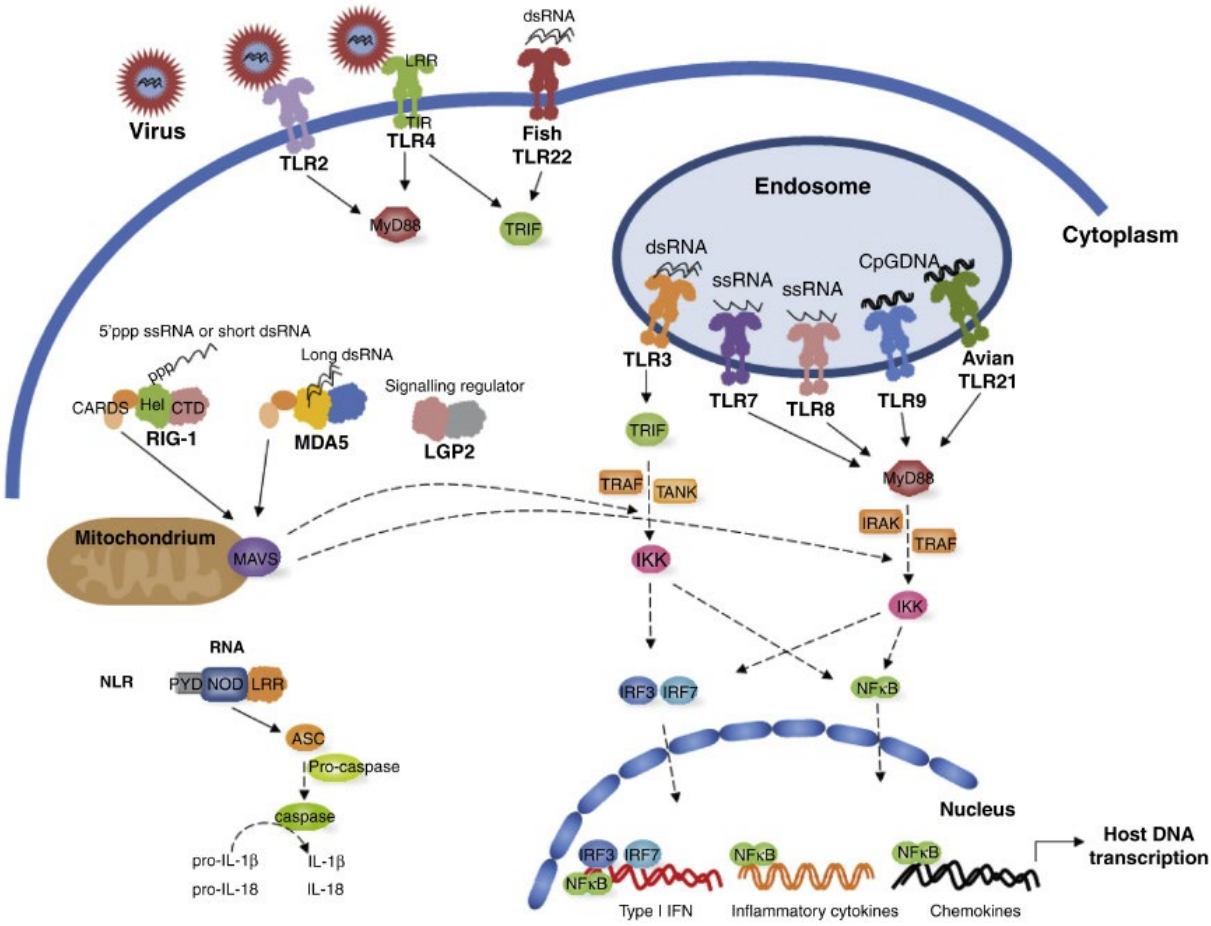

Figure 1.1 Schematic representation of NLRs, TLRs and RLRs viral signaling pathways in vertebrates. TLRs: TLRs recognize viral PAMPs, leading to activation and downstream signaling via MyD88 or TRIF adaptor molecules. Activated MyD88 and TRIF interacts with IRAK, TRAF, TANK and IKK proteins leading to activation of NF-kB and IRF3/7 transcription factors. NF-κB and IRF3/7 translocate to the nucleus leading to transcription of type I IFNs, proinflammatory cytokines and chemokines. **RLRs:** Upon RIG-I and MDA5 activation by viral RNA, they bind the adaptor MAVS, leading to NF-κB and IRF3/7 activation. LGP2 are proposed as regulators of RIG-I and MDA5. **NLRs:** NLRs that sense viral nucleic acids activate the adaptor ASC, inducing caspase activity. Catalytic active caspase cleaves pro-IL-1β and pro-IL-18 to their mature forms. (Figure from Zou, 2016).

1.4 Nucleotide-binding oligomerization domain (NOD)-like receptors (NLRs)

In mammals, NLRs play a vital role in protecting against infections by invading pathogens. In teleosts, NLR sequences have been found to be homologous to those of mammals, suggesting that they play a similar role (Zhang et al., 2018).

In mammals, NLRs are cytoplasmic receptors characterized by N-terminal effector-binding domain (EBD), a centrally located nucleotide-binding oligomerization domain (NBD or NACHT) and a C-terminal leucine-rich repeat domain (LRR) (Fig. 1.3). The EBD domain is less conserved and can comprise of a caspase activation and recruitment domain (CARD), pyrin domain (PYD), baculovirus inhibitor of apoptosis domain (BIR) or activation domain (AD). The LRRs are vital in ligand recognition and NLR activation and the NACHT domain plays a crucial role in NLR activation and regulation of inflammatory responses, whilst the EBD is responsible for interactions with adaptor molecules and downstream effector proteins (Zhang et al., 2018, Yu and Levine, 2011).

Figure 1.2 Schematic structure of NLRs. NLRs are intracellular receptors comprising of a C-terminal LRR domain responsible for ligand recognition, a central nucleotide-binding oligomerization domain (either NBD or NACHT) and a variable N-terminal domain (PYD, CARD, BIR or AD).

Based on the type of EBD domain, the NLR family in mammals can be divided into four subfamilies: NLRA (containing AD domain, including CIITA), NLRB (Containing BIR domain, including NAIP1-7), NLRC (containing CARD domain, including NOD1-3, IPAF and NOD27) and NLRP (containing PYD domain, including NLRP1-14) (Zhang et al., 2018, Zhu et al., 2013). The NLR family can also be grouped according to their physiological functions: inflammasome-forming, reproductive and regulatory NLRs. Inflammasome forming NLRs are associated with interleukins and inflammatory cell death. Reproductive NLRs are associated with reproduction and embryogenesis, whilst the regulatory NLRs can function as either positive (NOD2) or negative (NLRX1) regulators in diverse signaling pathways (Yu and Levine, 2011, Zhang et al., 2018).

In teleosts, different NLRs have been described in several species including, zebrafish (*Danio reiro*), Atlantic salmon, goldfish (*Carassius auratus*), Japanese flounder (*Paralichthys olivaceus*) and lumpfish (Laing et al., 2008, Xie et al., 2013, Park et al., 2007, Pontigo et al., 2016, Larsen, 2019). Three distinct NLR subfamilies have been identified in zebrafish: NLRA (resembling NODs), NLRB (resembling NLRPs) and NLRC (containing 405 NLR genes unique to teleost fish, with some portions resembling mammalian NOD3 and NLRPs) (Zhu et al., 2013, Li et al., 2017). In lumpfish, NLRC3, NLRC5A, NLRCB, NLRX1, NOD1, NOD2 and CASP1 have been identified (Larsen, 2019). Challenge experiments with polyI:C have shown both mammalian and teleost NOD2 to be involved in antiviral response (Zou, 2016, Zhang et al., 2018, Sabbah et al., 2009).

1.5 Toll-like receptors (TLRs)

The TLRs family is the best understood of the PRRs, and the primary knowledge about TLRs in teleost fish is based on TLRs in mammals. Studies have shown that key features of fish and mammalian TLRs have high structural similarity, however fish TLRs also exhibit very distinct features due to their evolutionary history. The first teleost TLR to be identified was in goldfish in 2003 (Stafford et al., 2003), and since then the receptors have been identified in several fish species, including Japanese flounder, rainbow trout (*oncorhynchus mykiss*), yellow croaker (*Pseudosciaena crocea*), channel catfish (*Ictalurus punctatus*), Atlantic salmon, grass carp (*Ctenopharyngodon idella*) and lumpfish (Stafford et al., 2003, Aoki et al., 2013, Eggestøl et al., 2018, Hirono et al., 2004, Baoprasertkul et al., 2007, Kongchum et al., 2011, Lv et al., 2012, Tsujita et al., 2004).

TLRs in mammals and teleosts are transmembrane proteins anchored to the membrane, except for a soluble variant of TLR5 (TLR5S), forming homo-or heterodimers (Aoki et al., 2013). The receptors consist of an extracellular N-terminal domain responsible for PAMP recognition, a leucine-rich repeat (LRR), a transmembrane domain (TM) and a cytosolic Toll/interleukin 1 receptor (TIR) signaling domain at the C-terminus (Fig. 1.4). While the TIR domain is highly conserved across species, the LRR motifs present a high variability. The LRRs comprises of 20-43 residues including the sequence motif LxxLxLxxNxL (Jin and Lee, 2008, Matsushima et al., 2007). The 3D structure of several TLRs revealed that each individual LRR to form a loop and the juxtaposition of several LRR loops produces

a solenoid structure (Bell et al, 2003). Different insertions of LRRs in the N-terminal domain generate different conformations which are considered to be related to the specific PAMP recognition of TLRs (Takano et al., 2010, Aoki et al., 2013, Zou, 2016).

Figure 1.3 Schematic structure of TLRs. TLRs comprise of LRRs at the N-terminal responsible for ligand recognition, a transmembrane segment and a TIR-domain involved in signaling at the C-terminal.

Upon PAMP recognition in mammals, TLRs dimerize and activate intracellular signaling pathways via intracellular TIR-domain containing adapter molecules (Takano et al., 2010). Five essential TIR domain-containing cytosolic adapters exists including myeloid differentiation primary response protein 88 (MyD88), TIR domain containing adapter protein (TIRAP or MAL), TIR domain-containing adapter including interferon-β (TRIF or TICAM1), TRIF-related adapter molecule (TRAM or TICAM2) and sterile-alpha and armadillo motif protein (SARM) (Yu and Levine, 2011). When the TIR domain-containing adaptor proteins are recruited to the cytoplasmic portion of the TLRs, a signaling cascade is triggered leading to the production of proinflammatory cytokines and type I IFNs. In mammals, TLR3, 7, 8 and 9 recognize viral nucleic acids (Aoki et al., 2013). Upon recognition of viral PAMPs, TLR3 homodimerizes, while TLR8 (which, similar to TLR7 senses ssRNA) dimerizes with TLR7 or TLR9 (which recognize viral DNA) (O'Neill and Bowie, 2007).

In teleost, 22 TLRs have been identified including TLR1, 2, 3, 4, 5M (membrane bound), 5S (soluble), 7, 8, 9, 13, 14, 18, 19, 20, 21, 22, 23, 24, 25, 26, 27 and 28. Eleven of these are fish specific; TLR18-20, TLR22-28 and TLR5S (Wang et al., 2016, Takano et al., 2010, Palti, 2011). Amongst teleost TLRs, TLR 7, 8 and 9 recognizes ssRNA, while TLR3 and 22 recognizes dsRNA. Endosomal TLR3 and 22 signals solely via TRIF, whilst TLR7, 8 and 9 depend on MyD88 for signaling (Zou, 2016, Zhou et al., 2018). In addition to TRIF and MyD88, SARM and TIRAP have been identified in teleosts, including lumpfish (Eggestøl et al., 2018, Lunde et al., 2019). It is yet poorly understood how the TLR signaling pathway is regulated in teleosts

1.6 Retinoic acid inducible gene (RIG)-I like receptors (RLRs)

In mammals, RLRs are key cytosolic PRRs detecting viral PAMPs in virus-infected cells, pivotal for activation of IFN type I transcription (Onomoto et al., 2021). The family comprises of three receptors; RIG-I, Melanoma Differentiation Associated gene-5 (MDA5) and Laboratory of genetics and physiology (LGP2) (Nerbøvik et al., 2017, Aoki et al., 2013, Zou et al., 2009, Lazarte et al., 2019). All three receptors belong to the phylogenetically conserved DExD/H-box family of helicases possessing a common functional RNA helicase domain near the C-terminus and a C-terminal repressor (CTD) domain (Chen et al., 2017, Onomoto et al., 2021). RIG-I and MDA5 share a similar structure with the N-terminal region containing two tandem arranged caspase activation and recruitment domains (CARDs) involved in protein-protein interactions, which is not found in LPG2 (Fig. 1.5). While the helicase domain of RLRs is essential for dsRNA recognition, the CARD domains trigger activation of IFNs via interferon regulatory factor 3 (IRF3) and nuclear factor kappa-light-chain-enhancer of activated B cells complex (NF-κB) (Aoki et al., 2013, Ranjan et al., 2009, Workenhe et al., 2010, Rajendran et al., 2012).

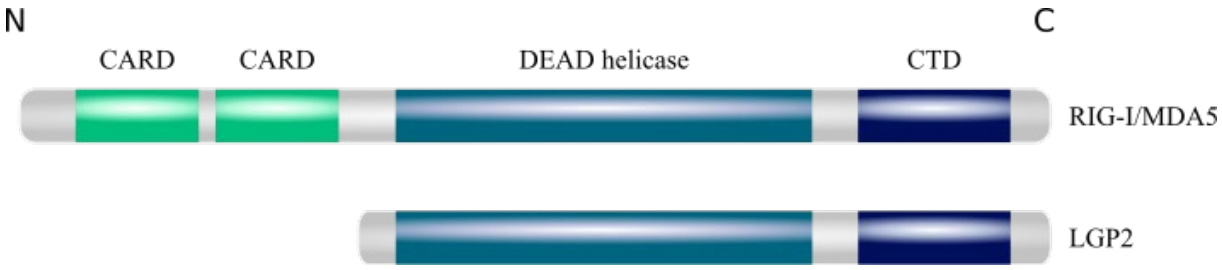

Figure 1.4 Schematic structure of RLRs. The RLR consist of an ATPase domain containing DExD/H box helicase and a CTD. RIG-I and MDA5 additionally possess two CARD domains near the N-terminus.

RIG-I is known to have a key role in recognizing dsRNA viruses discriminating host RNA from viral RNA based on the 5´phosphate of viral RNAs. Furthermore, RIG-I preferentially recognizes short dsRNA, whilst MDA5 recognizes long dsRNA (Rajendran et al., 2012). LGP2 is a regulatory protein shown to interfere with the binding process of RIG-I/MDA5 to viral RNAs. It was originally identified as a negative regulator of RIG-I through sequestration of RNA, but it has later been suggested that LPG2 in certain cases is a positive regulator of RIG-I and MDA5-mediated antiviral response and can potential enhance IFN production during viral infection (Chen et al., 2017, Yu and Levine, 2011).

Upon viral infection in mammals, the CARD domains of RIG-I/MDA5 interacts with the CARD domain of the adaptor molecule mitochondrial antiviral-signaling protein (MAVS) in a CARD-CARD-dependent manner (Workenhe et al., 2010). This interaction displaces NLRX1, a negative regulator that binds the CARD domain of MAVS, leading to MAVS dimerization (Yu and Levine, 2011). The dimerization recruits TRAF family members associated NF-κB activation binding kinases (TBK1), inhibitors of NF-κB (iκB) kinase (IKKe-i) and the IKK complex. Formation of this multi-protein signaling complex activates IRF3/7 and NF-κB. Homodimers of the phosphorylated IRF3 translocate to the nucleus and recruit the transcriptional coactivators p300 and cAMP response element binding (CREB) proteins to initiate IFN synthesis (Yu and Levine, 2011, Workenhe et al., 2010).

The RLR signaling pathway seems to be conserved across vertebrate species. In teleosts, MDA5 and LGP2 have been found in the genome of all fish species investigated. RIG-I however, has not yet been identified in species belonging to the superorder Acanthopterygii (Aoki et al., 2013, Zou et al., 2009).

1.7 Interferons (IFNs)

IFNs are inducible cytokines pivotal for first-line antiviral defense in vertebrates. IFN-activity was first identified in teleosts in 1965 but were not reported cloned until 2003 (Robertsen et al., 2003). Since then, IFN genes have been reported in numerous fish species, including zebrafish, grass carp, japanese flounder, Atlantic salmon, rainbow trout, goldfish, channel catfish, seabass (*Dicentrarchus labrax*), gilthead seabream (*Sparus aurata*), green spotted pufferfish (*Dichotomyctere nigroviridis*), Japanese pufferfish (*Takifugu rubripes*), medaka (*Oryzias latipes*), large yellow croaker, Nile tilapia (*Oreochromis niloticus*), Japanese eel (*Anguilla japonica*), black carp (*Mylopharyngodon piceus*), mandarin fish (*Siniperca chuatsi*), spotted gar (*Lepisosteus oculatus*), orange-spotted grouper (*Epinephelus coioides*) and stickleback (*Gasterosteus aculeatus*) (Aoki et al., 2013, Rajendran et al., 2012, Altmann et al., 2003, Kitao et al., 2009, Zou and Secombes, 2011, Ding et al., 2016, Gan et al., 2020, Hu et al., 2017, Huang et al., 2019, Huang et al., 2015, Laghari et al., 2018, Liu et al., 2019, Zou et al., 2021, Chen et al., 2014).

Based on gene sequence, protein structure and functional properties, mammalian IFNs are classified into three subgroups: type I, type II and type III. Type I and III trigger specific signaling pathways leading to activation of the innate immune defense against viral infections, whilst type II IFNs primarily promote cell mediated immunity (Gan, 2019, Zou and Secombes, 2011). In teleosts, only type I and II IFNs are identified, in which type I is involved in antiviral defense (Zou and Secombes, 2011).

Teleosts possesses multiple copies of the IFN genes, which are likely due to the teleost specific whole genome duplication (WGD) event (Liu et al., 2019, Liu et al., 2020). The gene copy number varies depending on the species; Atlantic salmon possesses 11 type I IFN genes (Robertsen, 2018), whereas zebrafish appears to possess four IFN genes (Zou et al., 2007). One of the characteristic features of fish type I IFN genes is the unique genomic organization, consisting of five exons and four introns, in which all four introns separating the coding region are in phase 0 (Zou and Secombes, 2011). This have led to the assumption that fish type I IFNs are homologous to mammalian type III IFNs, as these, but not mammalian type I, also are encoded by intron-containing genes with five exons and four introns (Workenhe et al., 2010, Gan et al., 2020). However, sequence analysis of fish IFNs suggest them to be homologous of mammalian type I IFNs as they possess two important sequence features conserved between fish and mammalian type I IFNα. This includes the cysteine pattern and the C-terminal CAWE motif. In 2011, the three-dimensional structure of zebrafish IFNs were determined, revealing that both zebrafish IFN1 and IFN2 possess typical type I IFN structure with a straight F helix. (Gan, 2019, Zou and Secombes, 2011, Hamming et al., 2011).

Based on conserved cysteine patterns, type I IFNs in teleosts can be further subdivided into three groups (I-III) (Fig. 1.6). Group I type I IFNs exists in alle teleosts, whilst group II and III are limited to certain species within Salmoniformes, Cypriniformes, Siluriformes and some Perciformes (Zou et al., 2021). Group I possess two conserved cysteine and is the most diversified group, further divided into the subgroups a, d, e and h. Group II and III possesses four conserved cysteines and are further divided into the groups b and c (group II) and f (group III) (Fig.6) (Liu et al., 2019). Salmonids appear to possess the most complex type I IFN repertoire, containing IFNa, b, c, d, e and f, whilst the type I IFN repertoire in most fish species appear to only contain the three subgroups a, c, and d. IFNh is only reported in Perciformes, in which large yellow croaker (Ding et al., 2016), meagre

(Milne et al., 2018) and mandarin fish (Laghari et al., 2018) are shown possess IFNc, d and h indicating that Perciformes contain both group I and II type I IFN genes. Synteny analysis have revealed that teleost possess two IFN loci, linked to growth hormone (GH) or CD79B (Liu et al., 2019).

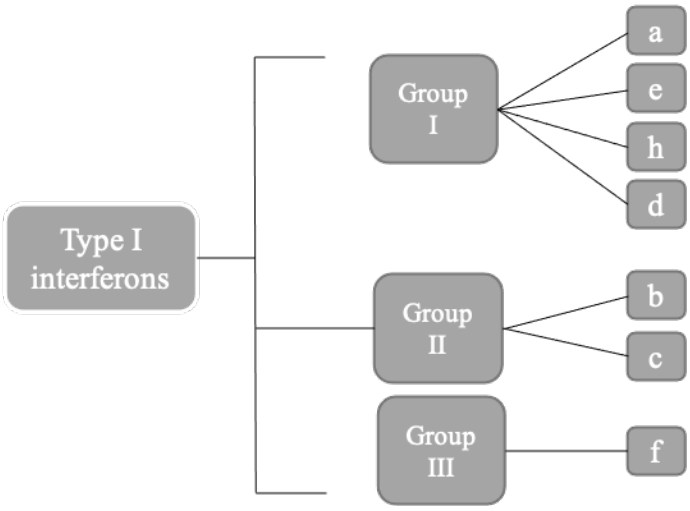

Figure 1.6 Schematic classification of type I interferons. Type I IFNs can be subdivided into group I, II and II based on conserved cysteines. Group I are further subdivided into a, e, h and d, group II into b and c and group III into f.

Generally, teleost type I group I IFNs appear to be expressed at low levels in most cell types and tissues and are upregulated upon viral infection, whilst group II type I IFNs are constitutively expressed at very low level and induced in specific leukocyte populations (Ding et al., 2016, Ding et al., 2019). In large yellow croaker *IFNh*, *IFNc* and *IFNd* were shown to be continuously expressed in all tissues examined, but with different levels of expression. *IFNc* and *IFNh* exhibited a higher level of transcripts post polyI:C stimulation, compared to *IFNd*. *IFNc* was also found to induce the expression of itself, as well as *IFNd* and *IFNh* (Ding et al., 2016, Ding et al., 2019). Similar results were also found in mandarin fish were all three *IFNh*, *IFNc* and *IFNd* were found to have a constitutive expression in all tissues examined, although relatively low level was observed for *IFNd*. PolyI:C stimulation provoked up-regulation of all three genes, but varying degree of expression in different organs/tissues (Laghari et al., 2018).

In mammals, binding of virus-derived nucleic acids to RIG-I, MDA5, TLR3, 7, 8 and 9 results in coordinated activation of the transcription factors IRF family, NF-κB and c-jun

(JNK)/authophagy12 (atg12) which subsequently leads to transcription of type I IFN genes (Kileng et al., 2008). In teleost, 12 members of the IRF family have been identified, in which 9 of them are orthologous of mammalian IRFs (Liao et al., 2016). Expression of type I IFNs results in the activation of janus associated kinase/signal transducer and activators of transcription (JAK/STAT) pathway. Type I IFN receptors have two subunits, interferon alpha and beta receptor subunit 1 (IFNAR1) and IFNAR2, which are associated with tyrosine kinase 2 (TYK2) and JAK1, respectively. Activation of IFNAR by type I IFN binding results in transphosphorylation and activation of TYK2 and JAK1 (Laghari et al., 2018). Subsequently, TYK2 phosphorylates IFNAR1, creating a docking site for STAT-2. STAT-2 is further phosphorylated by TYK2, recruiting STAT-1, which is then phosphorylated. The phosphorylated STAT-1/2 heterodimer then dissociate from the receptors and translocates to the nucleus to bind with unphosphorylated IRF9, generating interferon stimulated gene (ISG) factor 3 (ISGF3) (Pereiro et al., 2014). The ISGF3 complex then binds IFN-stimulated response elements (ISRE) present in the promoters of certain ISGs, thus initiating the transcription of ISGs (Workenhe et al., 2010). ISGs include ISG-15, Viperin, protein kinase R (PKR), oligo adenylat synthetase (OAS) and Myxovirus resistance protein (Mx) (Verhelst et al., 2013). Once ISGs are activated they inhibit cellular processes required by the virus to replicate and spread, thus initiate antiviral state in the host cell that is dedicated to fight off viral attacks (Sadler and Williams, 2008).

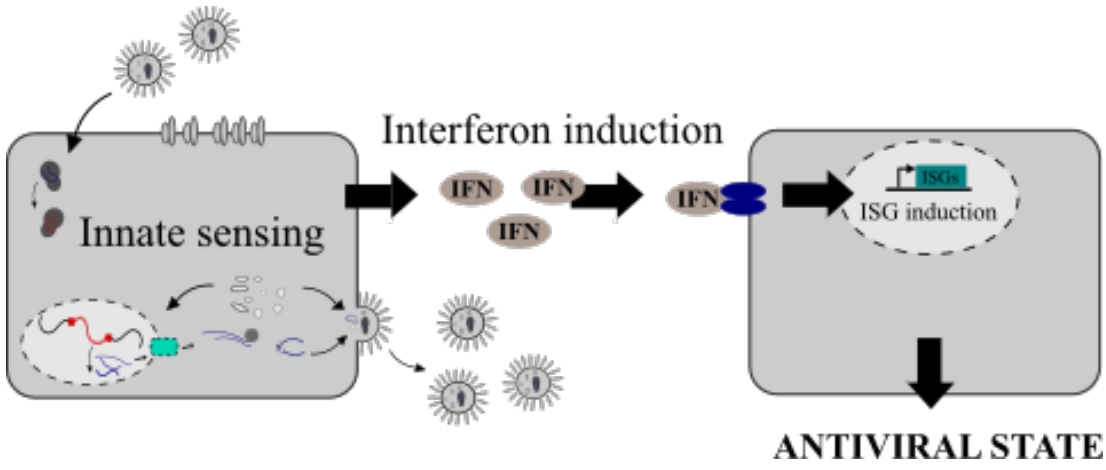

Figure 1.7 Innate sensing and induction of antiviral state in infected cells. Upon viral infection the innate immune system is triggered through PAMP recognition by PRRs. Activated PRRs induce signaling cascades leading to transcription of IFNs. IFN induce production of ISG such as MX. (modified from https://www.irim.cnrs.fr/index.php/en/researchh/teams/interferon-and-antiviral-restriction)

Analysis of teleost genomes have revealed presence of all key components of the JAK-STAT signaling pathway, including JAK1, TYK2, STAT1 and STAT2 (Stein et al., 2007, Zou and Secombes, 2011). However, in contrast to mammalian type I IFNs, fish type I IFNs seem to exert their function through two distinct receptors. Studies in zebrafish revealed type I group I IFNs to signal through a receptor composed cytokine receptor family B (CRFB)1 and CRFB5, whilst group II IFNs functions through CRFB2 and CRFB5 (Zou et al., 2021, Zhang and Gui, 2012).

1.9 Aim of study

Lumpfish is a relatively new species in the aquaculture, suffering from high mortality due to both bacterial and viral infections, and efficient vaccines to actual pathogens are urgently needed. To date, immunological studies in lumpfish has focused on antibacterial responses and there is currently little knowledge of its antiviral defense.

Therefore, the aim of this thesis was to study early antiviral responses in lumpfish and identify the key molecules involved, with particular emphasis on type I IFNs. This includes characterization of IFNs, both through bioinformatical analysis and *in vitro* and *in vivo* experiments. Furthermore, we aimed to study the IFNs role in antiviral immunity by investigating if recombinants IFNs were able to induce expression of the Mx protein *in vitro*.

Sub-objectives:

- Transcriptome-wide analyses of the RIG-I signaling pathway
- Characterize and subtype-determine type I IFN candidates
- Analyze basal expression of *IFNs* in nine tissues from lumpfish
- Examine *IFN* gene expression upon viral PAMP stimulation *in vitro* and *in vivo*
- Use recombinant IFNs to induce expression of Mx

2. MATERIALS

2.1 Solutions, media and buffers

2.1.1 Media for leukocyte isolation

L-15 (370 mOsm)
5% (v/v) H_2O
0.24 µg/ml NaCl
0.28 µg/ml $NaHCO_3$
0.066 µg/ml Glucose
95% (v/v) L-15 medium

L-15+ medium
10% (v/v) gentamicin
10 U/mL heparin stock-solution
15 mM HEPES
2 mM Glutamin
97% (v/v) L-15 (370 mOsm)

2.1.2 Buffers and solutions for gel electrophoresis

50 x TAE buffer
40 mM Tris
20 mM acetic acid
1 mM EDTA

10x TGS buffer
0.25 M Tris
1.92 M Glycine
1% (v/v) SDS

4x SDS sample buffer
62.5 mM Tris-HCl pH 6.8
24.7% (v/v) Glycerol
2% SDS
0.01% (w/v) Bromphenol Blue
5% (v/v) β-Mercaptoethanol

5x loading buffer for Agarose gel
0.25% (w/v) Bromphenol blue
0.1% (w/v) EDTA
30% (w/v) Glycerol

4% SDS-PAGE stacking gel
125 mM Tris-HCl pH 6.8
4% Acrylamide-Bisacrylamide
0.1% SDS
0.05% APS
0.001% (v/v) TEMED

12% SDS-PAGE resolving gel
375 mM Tris-HCl pH 8.8
12% Acrylamide-Bisacrylamide
0.1% SDS
0.05% APS
0.0005% (v/v) TEMED

2.1.3 Media and solutions for bacterial work

LB-media
25 g LB-Broth
1 L dH_2O

LB-agar
1L LB-media
12 g/L bacto agar
100 µg/mL Ampicillin

S.O.C medium
2% (w/v) Trypton
0.5% (w/v) yeast extract
10 mM NaCl
2.5 KCl
10 mM $MgCl_2$
10 mM $MgSO_4$
20 mM Glucose

TBS
1.7% (w/v) Pancreatic digest of casein
0.3% (w/v) Pancreatic digest of soybean
0.25% (w/v) Dextrose
2% (w/v) NaCl
0.25% (w/v) K_2HPO_4
1 L dH_2O

2.1.4 Media for autoinduction

50x 5052
25% (w/v) glycerol
2.5% (w/v) Glucose
10% (w/v) α-lactose

20x NPS
0.5 M $(NH_4)_2SO_4$
1 M KH_2PO_4
1 M Na_2HPO_4

5x PA-0.5G
1 mM $MgSO_4$
0.5% (w/v) Glucose
1x NPS
50 µg/mL Ampicillin
100 µg/mL Chloramphenicol

Zy
1% (v/w) N-Z casey plus
0.5% (v/w) yeast extract

Zyp-5052
92.8% (v/v) ZY
1 µM $MgSO_4$
1x 5052
1x NPS
50 µg/mL Ampicillin
100 µg/mL Chloramphenicol

2.1.5 Buffers for protein purification

Lysis/wash buffer
50 mM Tris-HCl pH 8.0
0.5 M NaCl
20% Glycerol
10 mM Imidazole

Lysis buffer w/ urea
50 mM Tris-HCl pH 8.0
0.5 M NaCl
20% Glycerol
10 mM Imidazole
8 M Urea

Elution buffer 1
50 mM Tris-HCl pH 8.0
0.5 M NaCl
20% Glycerol

Elution buffer 2
50 mM Tris-HCl pH 8.0
0.5 M NaCl
20% Glycerol
0.5 M Imidazole

4x Stripping buffer
400 mM EDTA
2 M NaCl
80 mM Tris-HCl pH 8.0

8x Ni-buffer
400 mM $NiSO_4$x $6H_2O$

2.2 Fish

Table 2.1 Provider of fish

Supplier	Location	Fish
Vest Aqua base	Norway	Farmed and unvaccinated lumpfish

2.3 Apparatus and instruments

Table 2.2 Apparatus and instruments

Supplier	Instrument	Function
Thermo Fisher	NanoDrop 2000	Nucleic acid concentration measurement
	Applied biosystems 2720 thermal cycler	cDNA synthesis and PCR
	Thermo French press	Cell disruption
	Heraeus biofuge pico	Centrifugation
BioRad	CFX96™ Real time with C400 touch thermal cycler	qPCR
	C100 touch Thermal cycler with CFX96 Real-time system	qPCR
	PowerPac basic	Power supply for gel electrophoresis
	Gene pulser Electroporator with pulse controller	Electroporation
	Mini-ProTEAN tetra cell	SDS-PAGE chamber
	GelDoc™ XR+	Gel imaging
Pharmacia	FPLC system	Protein purification
	Pump P-500	Protein purification
	Controller LCL-501 plu	Protein purification
	Frac-100	Protein purification
Beckman Coulter	Allegra X-IR centrifuge	Centrifugation
	Avanti J-26XP with JLA 9.100 rotor	Centrifugation
MP biomedicals	FastPrep-24 5G homogenizator	Tissue homogenization
Miltenyi Biotec	GentleMacs dissociator	Tissue homogenization
Innovatis	CASY cell counter	Cell count
Syngene	G: Box GelDoc	Agarose gel analysis
UVP	High performance ultraiolet transilluminator	UV-light
Labnet	Accublock™	Heating block
Eppendorf	Thermomixer comfort	Heating bock with shaking
Sonics	Vibra-Cell™	Sonication (cell disruption)
AA Hoefer	HE33 mini horizontal submarine unit	Agarose electrophoresis chamber

2.4 Commercial reagents, materials and kits

Table 2.3 Commercial reagents, materials and kits

Supplier	Name	Function	Cat. No
Sigma Aldrich	Gene elute Mammalian total RNA Kit	RNA isolation	SLBR6346V
	DNase I Amplification grade	DNA removal	SLBZ1532
	SYBR green jumpstart ™ Taq	qPCR	SLCF3807
	GeneElute plasmid mini prep	Plasmid isolation	SLBM2936V
	GeneElute PCR clean-up	PCR prod. isolation	040M6153
	dNTP mix	PCR	D7952
BioRad	SDS-PAGE standard, low range	SDS-PAGE analysis	161-0304
	Gene Pulser Cuvette	Electroporation	165-2086
	Silver Stain plus™	Staining of SDS-gel	161-0449
Quantabio	qScript cDNA synthesis kit	cDNA synthesis	66139688
BD	BD® Vacutainer Heprain	Blood collection	367869
MP biomedicals	Lysing Matrix S, 2mL tube	Tissue sampling	6925-500-91500
Omega Bio-tek	E.N.Z.A Gel extraction kit	Gel extraction	D25000104 111830121980
Invitrogen	1-kb + DNA ladder	Agarose gel analysis	10787018
Thermofisher	BigDye™ terminator V3.1 cycle sequencing kit	Sanger sequencing	4336921
GE healthcare	Chelating sepharose™ fast flow	Protein purification	17-05-7052

2.5 Enzymes and reaction buffers

Table 2.4 Enzymes and reaction buffers

Supplier	Name	Use	Cat. No
Thermo Scientific	5x HF buffer	Amplification of genes for cloning	00781042
New England Biolabs	HF DNA Phusion polymerase	Amplification of genes for cloning	0031303
	10x NEW buffer 4	Restriction digestion	0030906
	XhoI	Restriction digestion	0550904
	NdeI	Restriction digestion	0291003
	T4 DNA ligase ligation buffer	Ligation of insert into vector	10069975
	T4 DNA ligase	Ligation of insert into vector	10064879
Finnzymes	DNAzyme	PCR verification	F-501L
	DNAzyme reaction buffer	PCR verification	F-511

2.6 Primers, plasmids and cells

Table 2.5 plasmids used for cloning and protein expression

Supplier	Plasmid	Cat. No
Sigma-Aldrich	pET21a (+) DNA - Novagen	69740

Table 2.6 Bacterial strains used for cloning and protein expression

Supplier	Name	Function	Cat. No
Agilent	BL21-Codon plus (DE3)-RIL	Protein expression	230240
Sigma-Aldrich	BL21(DE3) pLyS	Protein expression	69451-M
Invitrogen	TOP10 One shot ™ cells	Plasmid growth	1631295

Table 2.7 Primers for qPCR, cloning and sequencing

Gene	Sequence (5´-3´)	Application
RPS20	F, GGAGAAGAGCCTGAAGGTGAAG	qPCR
RPS20	R, GAGTTTTCCTGGTGGTGATGC	qPCR
IFNh	F, TCTCTGACTCTCATCCAACACATG	qPCR
IFNh	R, GAAAAGACACTGGACTCTCCTCATC	qPCR
IFNc	F, CCTTTCCAGACTCCGCCTTCCCTA	qPCR
IFNc	R, TCCGCTCCTTGCAGTGACTCATACA	qPCR
IFNd	F, AGCCACGGCCACAAGAAGAAGAAC	qPCR
IFNd	R, GCCCATTTGCTCCAGGATGTGTGA	qPCR
IFNh	F, GCGGACATATGATCAGCTGGACCAGCCTGCTT	Cloning
IFNh	R, CCCCTCGAGGTGACAGAAGAGCATCTGTTTCGGAGT	Cloning
IFNc	F, GCGGACATATGACGCTGTCTTCAGTCGTCCTCGTG	Cloning
IFNc	R, CCCCTCGAGGTGGGCATGTCTCCAGGTGAAACA	Cloning
IFNd	F, GCGGACATATGCTCCGCAGGATGTTGTTGGTGTTC	Cloning
IFNd	R, CCCCTCGAGGTTGGTGAGTAGAGATGAAGCCAGCTG	Cloning
pET11a	F, CGACTCACTATAGGGGAATTGTG	Sequencing
pET11a	R, CAAGGGGTTATGCTAGTTATTGC	Sequencing

2.7 In vitro *stimulants*

Table 2.8 *In vitro* stimulants

Supplier	Name	Cat. No
Invivogen	PolyI:C	PIC-39-12
	R848	848-39-03
Duncan J. Colquhoun(NVI)*	Whole bacteria (*Vibrio anguillarum* serotype 01)	

*The Norwegian Veterinary Institute

2.8 Chemicals and reagents

Table 2.9 Chemicals and reagents

Supplier	Name	Formula	Cat. No
Sigma Aldrich	L-15		SLBR6346V
	2-Mercaptoethanol		SLBV2753
	RNA later		MKCG4668
	Acetic Acid	CH_3COOH	SZBF22020V
	Ethylenediaminetetraacetic acid	EDTA	BLBW7247
	Calsium Chloride	$CaCl_2$	05210071
	99% Glycerol		SHBG0744V
	Ampicillin Sodium salt		116K1864
	Heparin		SLCCY4711
	Sodium bicarbonate	$NaHCO_3$	50H-01357
	D-(+)-Glucose		G8270
	Hepes		RNBD9762
	Nuclease and DNase free water	H_2O	RNBH3181
	Magnesium Chloride	$MgCl_2$	SZB92510
	Magnesium sulfate	$MgSO_4$	BCBB1371
	Trizma base		T1503
	α - Lactose		5989-81-1
	Disodium hydrogen phosphate	Na_2HPO_4	10028-24-7
	N-Z casey plus		N4642
	Hydrogenchloride	HCl	258148
	Imidazole		I202
	Nickel sulfate hexahydrate	$NiSO_4*6H_2O$	N4882
	Glycine		56-40-6
	Sodium dodecyl sulfate	SDS	151-21-3
	N,N´-metylenebisacrylamid		01709
	Tetrametylethylenediamine	TEMED	T9281
	Ammonium persulfate	APS	A3678
	Chloramphenicol		C-0378
Biowhittaker	Gentamicin sulfate		0000236697
	Glutamin		9MB054
	Phosphate-buffered saline	PBS	000786588
	Ammonium sulfate	$(NH_4)_2SO_4$	A4418
BD	Bacto agar		3092065
	Yeast extract		212750
	Tryptic Soy broth medium	TBS	211825
Merck	Bromphenol blue		L631122
	Urea	$CO(NH_2)_2$	K31980287
MoBio	LB-Broth		LB15F4
Lonza	SeamKem Agarose		AG918L

GE healthcare	Percoll		10266569
Biotium	GelRed		19G1205
NE Biolabs	Bis(trimethylsilyl)acetamide	BSA	0100901
VWR	Sodium Chloride	NaCl	18C014121
Fluka	Potassium dihydrogenphosohate	KH_2PO_4	7079054307003
Honeywell	Methanol	CH_3OH	32213

2.9 Software

Table 2.10 Software

Name	Function	Supplier / Developer
GeneSnap	Imaging of agarose gels	Syngene
UGENE	Multiple sequence alignment	Unipro
MegaX	Multiple sequence alignment	MEGA
jPRED v.4	Secondary structure elements prediction	jPRED
Genomicus v100.01	Synteny analysis	Genomicus
BLAST	Sequence analysis	NCBI
Pymol	Protein visualization	Schrödinger
Inkscape	Creating figures	Inkscape
Swiss-model	Protein structure prediction	Expasy
SignalP-0.5	Signal peptide prediction	SignalP
KEGG	Pathway analysis	Kanehisa laboratories

3. METHODS

The main goal of this thesis was to identify and characterize type I IFNs in in addition to study early antiviral responses in lumpfish, both through bioinformatical analyses and *in vivo* and *in vitro* stimulation experiments.

3.1 Bioinformatical analysis

Transcriptome analyses of RIG-I was performed in Kyoto Encyclopetida of Genes and Genomes (KEGG) with differential gene expression (DEG) data on RNA sequencing data of lumpfish head kidney leukocytes (HKL) exposed to polyI:C (data, Haugland´s lab). The longest DEG transcripts 24 hours post exposure (hpe) to polyI:C were used to generate the pathway if several transcripts were present.

IFN type I candidates were searched for in the above mentioned RNA sequencing data set in addition to RNA sequencing data from lumpfish HKL exposed to *V. anguillarum* O1 (Eggestøl et al., 2018) (Array Express: E-MTAB-6388). Three lumpfish *IFN* candidates were identified. The identities of the predicted amino acid sequences were predicted by Local Alignment Search Tool (BLAST) search using default parameters on the National Center for Biotechnology Information (NCBI) web site. Expasy was used to predict molecular weight and isoelectric point (https://web.expasy.org/compute_pi/). To scan for domains, InterProScan was performed. Selected species were used to generate a multiple sequence alignment (MSA) with MUSCLE in the UGENE program. A phylogenetic tree was conducted using selected sequences of characterized type I IFNs from fish, by the neighbour-joining method using the MEGAX program. The tree was bootstrapped 1,000 times and evolutionary distances were computed using the JTT matrix-based method. Synteny analysis of type I IFN loci was performed using Genomicus (database version 101.01) and the latest versions of genomes for zebrafish, stickleback and lumpfish, were retrieved from NCBI. Prediction of protein structures was conducted with Swiss-Model and visualized by Pymol.

3.2 Rearing conditions

Lumpfish were kept at the rearing facilities at the Aquatic and Industrial Laboratory (ILAB), Bergen High-Technology Centre, Bergen, Norway. The fish were kept under normal optimal rearing facilities at a temperature of 8-9°C, salinity of 34% and 12:12 h

light:dark with water flow of 300-400 L per hour and the outlet water had a minimum of 77% oxygen saturation. The fish were fed with 3 mm Amber Neptun pellets (Skretting).

3.3 Tissue sampling and homogenization

Lumpfish, with an average size of 366.3 ± 54.4 gr and 18.5 ± 1.5 cm (n=6), were randomly selected and killed by a sharp blow to the head. Tissue samples from HK, spleen, gill, liver, thymus, midgut, hindgut, skin and muscle with an average weight below 40 mg was dissected out aseptically from each fish. The tissue samples were incubated in 500 µL RNA later overnight and transferred to Lysis buffer supplemented with 1.6% (v/v) DTT. Homogenization of the tissue samples was performed in FastPrep Tubes containing SS metal beads lysing matrix with FastPrep-24 5G homogenizator.

3.4 Isolation of leukocytes

For *in vitro* stimulation, HK samples were aseptically dissected from lumpfish with an average size of 332.7± 22.2 gr and 17 ± 0.4 cm (n=4) before HKLs were isolated using discontinuous Percoll gradients as previously described (Haugland et al., 2012). HK tissue was transferred to GentleMACs tubes containing 3 mL L-15+ and homogenized by GentleMACS Dissociator using program D x 1. The cell suspensions were placed in centrifugation tubes containing 3 mL 1.070 g/mL Percoll overlaid with 2.5 ml 1.050 g/mL Percoll, before centrifugation (400 g, 40 min). The leukocytes were harvested from the interface between the Percoll density layers and washed in L-15+ medium followed by centrifugation (200 g, 10 min). The pellets were resuspended in 0.5 mL L-15+ medium before cell number, aggregation factor and viability were determined using CASY cell counter according to the manufacture's procedure.

3.5 Culturing of **Vibrio anguillarum**

To stimulate lumpfish HKLs with bacteria, *V. anguillarum* sereotype 01 was cultured in tryptic soy broth (TSB) medium containing 2% NaCl. It was grown at 20°C/200 rpm until late log phase, before centrifuged (13000 g, 2 min), washed once in phosphate-buffered saline (PBS) and resuspended in L-15+ medium.

3.6 In vitro *stimulation experiment*

Leukocytes (5 x 10^6) were added per well in a 24-well plate and stimulated with the following immunostimulants; 100 µg/mL PolyI:C (synthetic dsRNA), 10 µg/mL R848 (synthetic ssRNA), *V. anguillarum* (Multiplicity of infection (MOI) 1:10) or L-15+ only (unstimulated control) in a total volume of 500 µL. The plates were incubated at 15°C for 4 and 24 hours, before centrifugation (200 g,10 min). The medium was removed, the cells were resuspended in 0.5 mL lysis solution containing 1.6% (v/v) DTT and stored at -80°C.

3.7 In vivo *stimulation with polyI:C*

Farmed unvaccinated lumpfish with an average size of 32.1 ± 3.4 gr and 8.4 ± 0.4 cm (n=24) were either injected with 100 µL 1 mg/mL polyI:C solubilized in phosphate-buffered saline (PBS) or 100 µL PBS as control. HK (35.7 ± 10.5 mg) and spleen (30.2 ± 8.4 mg) were aseptically dissected from the fish 6 and 24 h post injection, transferred to FastPrep Tubes containing SS metal beads and 0.5 mL lysis buffer supplemented DTT and homogenized as described in 3.3.

3.8 RNA isolation, quantification and quality assessment

Total RNA was isolated from tissue samples and leukocytes using Sigma GenElute Mammalian Total RNA kit and treated with DNase I according to the manufacture's instruction. Briefly, the lysate was filtered using a filtration column, mixed with equal volume of 70% EtOH before transferred to GeneElute Binding column for centrifugation. Centrifugation was repeated with wash solution 1 in addition to two washing steps with washing buffer 2 supplemented with EtOH. Elution of RNA was performed with DNase and RNase-free water heated up to 70°C and RNA concentration was determined using Nanodrop spectroscopy. RNA was thereafter DNase I treated with a maximum of 2500 ng RNA per 10 µL DNase reaction. All centrifugation steps were carried out at maximum speed. To analyze the integrity of the RNA, 200 ng RNA in 1x loading buffer was run on an 1% agarose gel stained with GelRed in 1x TAE buffer at 80 V for 40 min. 1 Kb plus DNA ladder was used as molecular marker.

3.9 cDNA synthesis

Isolated RNA was reverse transcribed into cDNA using Sigma qScript^{TM} cDNA synthesis Kit according to the manufactures instructions, using maximum 1000 ng isolated RNA in 1x qScripts buffer and reverse transcriptase (RT) (samples without RT served as control) to a total volume of 20 µL. Incubation was performed at 22°C for 5 min, followed by reverse transcription at 42°C for 30 min before inactivation of RT at 85°C for 5 min. All incubations were performed in Applied biosystems 2720 Thermal cycler.

3.10 Quantitative real-time PCR (qPCR)

qPCR was carried out in C1000 Thermal cycler with CFX Real-time system, using 1x SYBR green JumpStart Taq Ready Mix kit, 20 ng cDNA (2 ng for the reference gene), 0.5 µL nuclease and salt free water and 10 mM gene specific primers under the following conditions: 5 min at 94 °C, followed by 40 cycles at 94°C for 15 sec, 60°C 1 min before 1 cycle at 60°C for 5 sec. All reactions were run in triplicate in a 96-well plate. Reactions without template (NTC) and cDNA reactions without reverse transcriptase (-RT) served as negative control to ensure that the primers did not bind non-specifically and that reagent were not contaminated. Primer sequences are listed in Table 2.7.

Data were analyzed using ΔΔCq method (Equation 1), as described in (Eggestøl et al., 2020). For all gene expression calculations, the housekeeping gene RSP20 was used as reference gene. For the gene expression analyses in normal tissue, mean normalized expression (MNE) values were folded relative to muscle (set to 1). In the *in vitro* and *in vivo* challenge experiments MNE values were folded relative to unstimulated control (which was set to 1).

$$\text{Equation 1: } \Delta\Delta Ct_{xy} = \frac{\frac{E_{\text{target}}{}^{x}}{E_{reference}{}^{y}}}{\frac{E_{target}{}^{x}}{E_{reference}{}^{y}}}$$

A standard curve for the three IFN genes was generated using 2-fold serial dilution of cDNA in three parallels (100 ng – 0.2 ng). Regression analysis, standard curve slopes of CT values versus log quantity and amplification efficiency E were calculated in qGENE (Muller et al., 2002).

3.11 Statistics

All three qPCR datasets were analyzed by two-way ANOVA in SigmaPlot (version 14.5) on log10 transformed data followed up by Tukey´s hones square difference post hoc test. The p values refer to the probability that the statistical summary of the population is equal or more extreme than the observed values of the sample, given that the null hypothesis is true and is considered significant when $p<0.05$. Statistical significance is indicated by: ***=$p<0.001$, **=$p<0.01$ and *=$p<0.05$.

3.12 Molecular cloning

3.12.1 Preparation of competent cells

E. coli BL21(DE3) cells were made chemical competent by treatment with calcium chloride ($CaCl_2$) to facilitate attachment of plasmid DNA to the cell membrane. BL21(DE3) cells (0.2 mL) were grown in 50 mL LB-medium at 37°C / 200 rpm. When log-phase was reached, the cells was centrifuged (4200 g, 15 min) before the pellet was resuspended in 25 mL ice-cold 0.1 M $CaCl_2$ solution and incubated on ice for 15 min. The resuspended pellet was centrifuged (4200 g, 15 min) followed by resuspension of the pellet in 2 mL ice-cold 0.1 M $CaCl_2$ solution with 400 µL 100% glycerol. The competent cells were stored at -80°C in 998 µL aliquots.

3.12.2 Plasmid preparation

To isolate the cloning vector pET21a, 0.2 mL of cells harboring the plasmid was grown in 20 mL LB-medium supplemented with 100 µg/mL ampicillin overnight (ON) at 37°C/200 rpm. Sigma´s plasmid mini-prep kit was used to isolate the plasmid according to the manufacture's description. Briefly, 3 mL ON culture was centrifuged (12000 g, 1 min) followed by resuspension of pellet in 200 µL lysis solution and addition of 350 µL neutralization solution. The solution was centrifuged (12000 g, 10 min) before the column was prepared by addition of 500 µL column preparation solution followed by centrifugation (12000 g, 1min). The supernatant was loaded onto the column and centrifuged (12000 g, 1 min), before two washing steps was performed. The plasmid was eluted by addition of 100 µL elution before centrifugation (12000 g, 1 min).

3.12.3 Amplification of **IFNh** *and* **IFNc** *for cloning into pET21a*

To amplify the *IFNh* and *IFNc* cDNA, PCR was performed. The reaction was performed with 47% (v/v) dH_2O, 1x HF buffer, 10 mM gene specific primers, 20 ng template, 1% (v/v) Phusion polymerase and 2% (v/v) 10 mM dNTP under the following conditions: 1.5 min at 98 °C, followed by 35 cycles at 98°C for 15 s, 69°C for 30s and 72°C for 30s before 1 cycle at 72°C for 1 min. The primer sequences are listed in Table 2.7.

3.12.4 Purification of PCR products

The PCR product for *IFNh* was purified using Sigma GeneElute PCR clean-up kit according to the manufacture´s description. Briefly, the column was prepared by addition of 500 µL column preparation solution followed by centrifugation (12000 g, 30s). 5 volumes of binding solution were added to 1 volume of PCR product and mixed well, before transferred to spinning column and centrifuged (12000 g, 1 min). The column was washed with 500 µL wash solution, before IFNh was eluted by addition of 50 µL elution solution followed by centrifugation (12000 g, 1 min). DNA concentration was measured using Nanodrop spectrophotometer.

3.12.5 Gel extraction

IFNc was run on an 1% agarose gel, before gel extraction was performed with E.Z.N.A Gel extraction kit-spin protocol according to the manufacture´s description. Briefly, the appropriate band was excised from gel out using scalpel before weighted. 1 volume of binding buffer was added to 1 volume of gel before incubated at 60°C for 7 min. A maximum of 700 µL of agarose solution was added to the spin column and centrifuged (10000 g, 1 min). 300 µL binding buffer was added and centrifuged (12000 g, 1 min) before 2 washing steps was performed with 700 µL SPW wash buffer. Elution was performed with 30 µL elution buffer. DNA concentration was measured using Nanodrop spectrophotometer.

3.12.6 Restriction digestion and ligation

To insert PCR products into the cloning vector, both *IFN* cDNA sequences and plasmid were treated with XhoI and NdeI. The restriction digestions were performed as described in Table 3.1 at 37ºC for 4 hours. As a control, pET21a was cut with only one enzyme at the time.

Table 3.1 Restriction digestion of IFNh and IFNc

Components	pET21a-XhoI	pET21a-NdeI	*IFNh*	*IFNc*	pET21a
dH_2O (µL)	10	10	4	-	-
10x buffer (µL)	2	2	6.5	3.5	6.5
BSA (1:10) (µL)	2	2	6.5	3.5	6.5
PCR product/plasmid (µL)	5	5	48	28	52
XhoI (µL)	1	-	5	2.7	5
NdeI (µL)	-	1	5	2.7	5

Following restriction enzyme cutting, plasmid and PCR product were purified using Sigma´s PCR clean up kit, as described in section 3.11.4 and DNA concentration was measured with Nanodrop spectrophotometer.

The ligation reaction was performed with 50% (v/v) insert, 25 % (v/v) vector, 15% (v/v) ligation buffer and 10% (v/v) T4 DNA ligase at 16 °C over night (ON=.

3.12.7 Transformation

For plasmid preparation, Top10 chemically competent cells were transformed with the ligation mix pET21a-*IFNh* and pET21a-*IFNc* constructs through heat shock transformation. The cells were transformed with 5 µL of the respective plasmid constructs by 30 min incubation on ice followed by heat shock at 42°C for 30s. The cells were incubated on ice for 2 min followed by incubation with 250 µl SOC medium at 37°C/225 rpm for 1h. 50 and 200µL of the cells were spread out on LB agar plates supplemented with 100µg/mL ampicillin. The plates were incubated at 37°C ON.

A single colony of *E. coli* expressing pET21a-*IFNh* and pET21a-*IFNc* was used to inoculate a start culture of LB-media supplemented with 100 µg/mL ampicillin, which was left to grow ON at 37°C/220 rpm.

3.12.8 Colony PCR and plasmid isolation

To verify if the plasmids contained the desired insert, colony PCR was performed. The PCR was carried out with 1x DNazym buffer, 10 µmol of the gene specific primers, 1U DNazyme, 0.22 mM dNTP and dH_2O to a final volume of 10 µL under the following conditions; 94°C for 10 min followed by 35 cycles at 94°C for 30 s, 55°C for 30s and 72°C for 1.5 min before 1 cycle at 72 °C for 10 min. The PCR products were analyzed on an 1% agarose gel before plasmid mini-prep was performed according to the manufacture's description. Primers are listed in Table 2.7.

3.12.9 Sanger sequencing

Sequencing of pET21a-*IFNh* and pET21a-*IFNc* plasmids was performed to verify the sequence of the insert, following the BigDye v.3.1 protocol. Briefly, template (150 ng) was supplemented with 3.3 pmol pET21a forward and reverse primer, 10% (v/v) BigDye, 1% (v/v) sequencing buffer and dH_2O to a total volume of 15 µL, before the PCR was carried out under the following conditions: 96°C for 5 min followed by 35 cycles at 96°C for 10 sec, 50°C for 15 sec and 60°C for 4 min. 10µL dH_2O was added to the samples before analysis at the seq. lab, UiB.

3.13 Protein expression and purification

3.13.1 Transformation and expression of IFNc and IFNh recombinant proteins

IFNh and *IFNc*-pET21 were added to BL21 (DE3) chemically competent cells and BL21-Codon plus (DE3) electrocompetent cells, before 30 min ice incubation. The BL21 (DE3) cells were heat-shocked as previously described, while BL21-codon plus (DE3) was subjected to electroporation. Electroporation was applied under the following conditions: 2.5 bV, 200 Ω and 25 µF to enable uptake of plasmid DNA. After electroporation the cells recovered in 250 µL SOC medium at 37°C /220 rpm for 30 min before left to grow ON on LB-Agar plates w/ ampicillin (100 µg/mL) overlayed with 100 µg chloramphenicol at 37°C. A single colony was used to inoculate a starter-culture of PA-0.5G medium, which was left to grow ON at 37°C/250 rpm. Bacterial growth and protein expression occurred in 1L ZYP-5052 medium supplemented with 10% PA-0.5G start culture, ON at 37°C /220 rpm.

3.13.2 Cell lysis

Bacteria were harvested by centrifugation (7000 g, 4°C, 20 min) and the cell pellet resuspended in lysis buffer both with and without urea (1 mL/g pellet). Cells were then lysed by French press twice at 900 psi followed by sonication (30% amplitude, 10 sec on/10 sec off, 3 min), centrifuged (5500 g, 4°C, 1 hour). The cell extract (CE) was collected, and the supernatant was filtered twice (0.75 µm and 0.4 µm).

3.13.3 Chromatography purification

The affinity of the 6xHis-tag imidazole rings to Ni^{2+} ions was exploited when the IFNs was purified from CE, using FPLC affinity chromatography (Pharmacia) system. Non-specific proteins were eluted with wash buffer, before the IFNs were eluted by increasing concentration of imidazole (10-500 mM) in the elution buffer. Protein fractions were monitored by UV_{280} absorbance.

3.13.4 SDS-polyacrylamide gel electrophoresis (SDS-PAGE)

To evaluate if the purification was successful, samples from the CE and purification process were analyzed by SDS-PAGE. The samples and standard (SDS-PAGE standard low range, BioRad) was prepared by addition of SDS sample buffer prior incubation at 98ºC for 7 min. 10 µL sample and 6 µL standard was loaded onto a 12% separation gel (4% stacking gel) and ran at 190 V for 1hour. Proteins were stained with silver staining plus™ (BioRad) according to the manufacture's description. Briefly, the gels were fixated with fixative enhancer solution for 20 min, before washed twice with dH_2O for 10 min each. Staining was performed with staining solution until visible bands, before stopped by addition of 5% acetic acid for 10 min. The gel was visualized with GelDoc™ XR+.

3.14 Ethical statements

The present work with lumpfish was conducted according to the approved national guidelines and performed according to prevailing animal welfare regulation. Rearing of fish under normal, optimal conditions does not require ethical approval under Norwegian law (FOR1996-01-15 nr 23). The in vivo experiment was approved by Norwegian Food Safety Authority (FOTS ID 26432). All work in this master's thesis has been done on tissues and cells harvested from dead fish. Fish were sacrificed with a sharp blow to the head, which is an appropriate procedure under Norwegian law.

4. RESULTS

4.1 Transcript analysis of the RIG-I-like receptor (RLR) signaling pathway

The RLR family, including RIG-I, MDA5 and LGP2, of signaling PRRs play a pivotal role in early innate immune responses against viruses. To identify components of the RLR signaling pathway and early immune responses in lumpfish, transcriptome wide analysis of HKL exposed to polyI:C 6 and 24 hpe were analyzed. Most of the components involved in RLR signaling were identified in lumpfish, including MDA5, LGP2, IRF3, TANK, TAK1, NF-κB and TRAF6 (a complete list is given in table 4.1). Interestingly, RIG-I was not identified. The most upregulated transcripts 6 hpe were LGP2 (logFC 2.6), IRF3 (logFC 2.1) and iKKγ (logFC 1.0), whilst MITA (logFC 3.0), LGP2 (logFC 3.0), IRF3 (logFC 2.7) and MDA5 (logFC 1.4) were most upregulated 24 hpe. The most downregulated transcripts 6 hpe were DDX3X (logFC – 0.8), TAK1 (logFC -0.6) and iKKβ (logFC -0.6), similarly the most downregulated 24 hpe were TAK1 (logFC -0.8), DDX3X (logFC -0.8) and iKKβ (logFC 0.5) (Fig. 4.1). The identity of the transcripts highlighted with color was annotated by BLAST search against NCBI´s non-redundant database (Table 4.1).

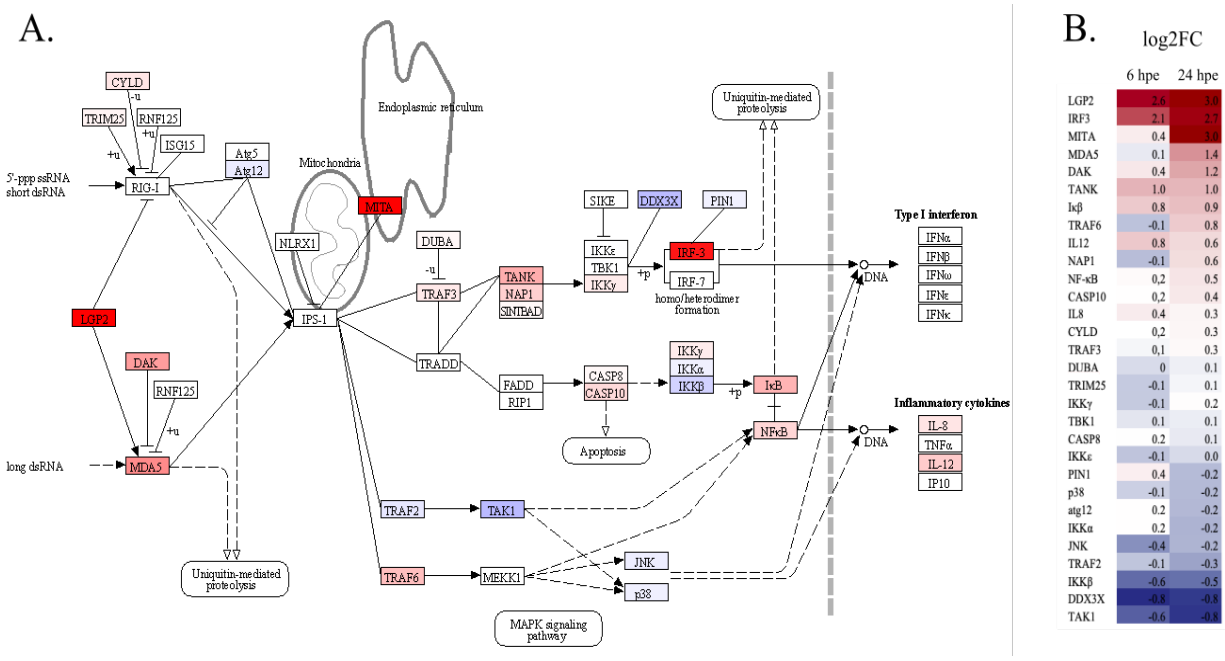

Figure 4.1 RIG-I like receptor signaling pathway (KEGG map 04622) in lumpfish. **A.** The colors of the boxes refers to the expression levels 24 hpe. White boxes represents molecules that are not present. **B.** DEG analysis of the signaling pathway 6 and 24 hpe. Exact values are given for each transcript and they are sorted by fold regulation at 24 hpe. The color gradient represents highly upregulated (dark red) to highly downregulated (deep blue).

Table 4.1 Proteins present in the RIG-I pathway in lumpfish annotated by BLAST search.

Trinity id	KEGG id	Annotation	Species	E-value
TRINITY_DN112355_c0_g1_i10	K12647	MDA5	*C. lumpus*	8e-121
TRINITY_DN120440_c10_g2_i6	K12649	LGP2	*C. lumpus*	0.0
TRINITY_DN111145_c2_g4_i17	K03174	TRAF3	*C. lumpus*	3e-65
TRINITY_DN117085_c2_g1_i2	K12650	TANK	*C. lumpus*	3e-153
TRINITY_DN47744_c0_g1_i1	K12651	NAP1	*C. lumpus*	2e-48
TRINITY_DN119285_c1_g5_i1	K07210	IKKγ	*C. lumpus*	0
TRINITY_DN108408_c0_g1_i2	K05410	TBK1	*C. lumpus*	1e-149
TRINITY_DN109791_c0_g1_i10	K05411	IRF3	*C. lumpus*	1e-96
TRINITY_DN114914_c3_g2_i3	K04398	CASP8	*C. lumpus*	1e-151
TRINITY_DN113815_c0_g1_i1	K04400	N.i.[1]		
TRINITY_DN171220_c0_g1_i1	K04467	IKKα	*S. dorsalis*	0.018
TRINITY_DN34730_c1_g1_i1	K07209	IKKβ	*C. lumpus*	5e-102
TRINITY_DN114493_c1_g1_i1	K04734	IκB	*C. lumpus*	8e-53
TRINITY_DN251843_c0_g1_i1	K02580	NF-κB -p105	*C. lumpus*	3e-32
TRINITY_DN118445_c4_g1_i9	K04735	NF-κB-p65	*C. lumpus*	4e-73
TRINITY_DN94956_c0_g1_i1	K03173	TRAF2	*C. lumpus*	0
TRINITY_DN113773_c1_g5_i2	K04427	TAK1	*C. lumpus*	5e-161
TRINITY_DN104040_c1_g1_i1	K03175	TRAF6	*C. lumpus*	8e-152
TRINITY_DN283601_c0_g1_i1	K04441	P38	*S. umbrosus*	0.048
TRINITY_DN106935_c0_g2_i6	K10030	N.i.[1]		4e-68
TRINITY_DN107617_c0_g1_i2	K05425	IL-12	*C. lumpus*	2e-74
TRINITY_DN340728_c0_g1_i1	K10652	TRIM25	*C. lumpus*	5e-111
TRINITY_DN114903_c0_g2_i6	K08601	CYLD	*C. lumpus*	0.0
TRINITY_DN111481_c1_g1_i8	K08336	ATG12	*C. lumpus*	1e-22
TRINITY_DN119693_c5_g9_i3	K12654	MITA	*C. lumpus*	6e-176
TRINITY_DN319478_c0_g1_i1	K11594	DDX3X	*C. lumpus*	0
TRINITY_DN120537_c3_g4_i3	K09578	PIN1	*C. lumpus*	3e-52
TRINITY_DN176051_c0_g1_i1	K12655	N.i.[1]		
TRINITY_DN116914_c1_g2_i7	K04440	JNK	*O. aureus*	2e-66
TRINITY_DN110967_c3_g1_i10	K07211	IKKε	*C. lumpus*	0

1 N.i. =ORF not identified

4.2 Identification and molecular characterization of lumpfish IFNs

No sequences in the lumpfish RNA seq data were automatically recognized as type I IFNs in the KEGG analysis. In depth search in the RNA seq data used for KEGG analysis, as well as in RNA seq data submitted to Array Express (E-MTAB-6388) identified three IFN candidates: TR62189|c0_g1|m.217665, TR62189|c0_g2|m.217669 and TRINITY_DN9568_g1_i. The sequences were further analyzed by performing a tBLAST-n search, confirming that they were IFNs. The top gene ID for all three sequences were predicted IFN sequences from lumpfish (Table 4.2).

Table 4.2 Overview of lumpfish IFN RNA seq data number and NCBI entry number

Trinity ID	NCBI entry	Annotation NCBI
TRINITY_DN9568_g1_i	XP_034394835	Interferon phi 1
TR62189|c0_g1|m.217665	XP_034396052	Interferon phi 3
TR62189|c0_g2|m.217669	XP_034414848	Interferon a3-like

To sub-type and sub-group the IFN sequences, bioinformatic characterization, phylogeny and synteny were performed. Based on the analysis described in the following section, lumpfish has IFNh, IFNc and IFNd.

4.3 Sequence and gene organization analysis of lumpfish type I IFNs

Sequence analysis revealed *IFNc* transcript to contain a 561 bp open reading frame (ORF), *IFNd* transcript a 540 bp ORF and *IFNh* a 686 bp ORF. The ORFs span all five exons and all intron door acceptor sites (indicated with black line) are consistent with the classical GT/AG splice junctions (Fig. 4.2)

A. IFNh

```
1      ctGCAGCCGCCATCTTCATCACTTTCGTCACCTTCATCATGATCAGCTGGACCAGCCTGC  60
          A  A  A  I  F  I  T  F  V  T  F  I  M  I  S  W  S  S  L
61     TTGTCTTCCTCCTCTGCAGCGCCGTGACCCCCAGCCTCGGCTGTGATTGGCTCAGAAACT  120
        L  V  F  L  L  C  S  A  V  T  P  S  L  G  C  D  W  L  R  N
121    ACGGTCACCTGAGCAACACCTCTCTGACTCTCATCCAACACATGgtgagtacataga//c  2360
        Y  G  H  L  S  N  T  S  L  T  L  I  Q  H  M
2361   ggaaataagggaataaagtgtaatctgttattgtgtctgtgtgtttcagGGCGGTCAGCT  2420
                                                      G  G  Q
2421   GACTGATGAGGAGAGTCCAGTGTCTTTTCCATACAGACTCTACCAATGCATAAAGAGCGA  2480
       L  T  D  E  E  S  P  V  S  F  P  Y  R  L  Y  Q  C  I  K  S
2481   TGAGgtaatcatcaatcaatcaatcatcaatctacatttcatttaaaacgacacttc//c  2720
       D  E
2721   ccactagATGGAGTCCCAGTTGGCTTTCGCCAGAGACAGTCTGGAGCTGATCGCTGGTCT  2780
                 M  E  S  Q  L  A  F  A  R  D  S  L  E  L  I  A  G
2781   CTATCGCCACGAGAACCGCTCCTCTGCTACCTGGGACACAGACGAGACCGAACGCTTCCT  2840
       L  Y  R  H  E  N  R  S  S  A  T  W  D  T  D  E  T  E  R  F
2841   GATGACCATCGACAGACAGACGGACGTCCTTAAGAGCTGCgtaagtagttagacactt//  9880
       L  M  T  I  D  R  Q  T  D  V  L  K  S  C
9881   gtcaaaacacttttttttgttcagGTGTCGACTCAAAGCCGAAAAGACAGCCGACTGAG  9940
                                  V  S  T  Q  S  R  K  D  S  R  L
9941   AAGATACTACCGGAGACTGGTGAAGAGTACTCTGTACCGCACTgtaagtacaagtat//t  11560
       R  R  Y  Y  R  R  L  V  K  S  T  L  Y  R  T
11561  tacagGGTGGTAGTCCTGCATCCTGGGAGCTGATCAGGAAGGAGAGTAAACTGCACCTGG  11620
             G  G  S  P  A  S  W  E  L  I  R  K  E  S  K  L  H  L
11621  ACCAGTTGGACCTGCTGGTGGGCTTCGTTGTGGACTCGGCGACAGACAGCAGGAGGCGCT  11680
        D  Q  L  D  L  L  V  G  F  V  V  D  S  A  T  D  S  R  R  R
11681  CTACAGACAGCAGGAGGCGCTCTACAGACAGCAGGAGGCGCTCTACAAACAGCAGGAGGC  11740
        S  T  D  S  R  R  R  S  T  D  S  R  R  R  S  T  N  S  R  R
11741  GCTCCACAGCGACTCCGAAACAGATGCTCTTCTGTCACTGA                    11781
        R  S  T  A  T  P  K  Q  M  L  F  C  H  S
```

B. IFNc

```
1      ATGACGCTGTCTTCAGTCGTCCTCGTGCTCCTGCAGGTCTACAGCCTTCACCGGATGGCG  60
         M  T  L  S  S  V  V  L  V  L  L  Q  V  Y  S  L  H  R  M  A
61     GTGGCCAAGCCGACCTGTTTGCTGGAAGGAAACATGGTCCAGTCGGCCCACCACCTTCTC  120
         V  A  K  P  T  C  L  L  E  G  N  M  V  Q  S  A  H  H  L  L
121    AGAGACCTGgtacgacctttgatctccgaaaagaaaactgcactcgtgttaacgaac//t  720
         R  D  L
721    ataaaggtgagtctttttcctttctgtcctgtagGGTGGTCCGTTTCCAATCCTCTGCCT  780
                                          G  G  P  F  P  I  L  C
781    GCCATACCGTGCCAACATCTCCTTTCCAGACTCCGCCTTCCCTACTGCAAAAGCCAATCA  840
       L  P  Y  R  A  N  I  S  F  P  D  S  A  F  P  T  A  K  A  N
841    CATTCAGgtaatcctctgacctgtcagacaatcacagagctgatttatgtcgaaaaggtt  900
       H  I  Q
901    tgtttaaaaattgtaactgacctctaattggttgcctgcagTGCCGCCGAGCATTAAGGG  940
                                                 C  R  R  A  L  R
941    TAGTGTATGAGTCACTGCAAGGAGCGGAACAGGTGTTTGAGGACCATGGGTTACCTGTCG  1000
        V  V  Y  E  S  L  Q  G  A  E  Q  V  F  E  D  H  G  L  P  V
1001   GAGGGGGCGGAGTCACCTGGGACCGCGAGAAGCTCAACCGATTCCGACACCTGCAGCACC  1060
        G  G  G  G  V  T  W  D  R  E  K  L  N  R  F  R  H  L  Q  H
1061   GACTGCTGGAGAAGGGAAGCTGTgtgagtacccgtctgtctgaacacctgtctatct//a  1480
        R  L  L  E  K  G  S  C
1481   taacctgtctctcacttttctccagTTGTCCAGTGTTGATTCAGGTGTTTTACCTTCTTAC  1540
                                 L  S  S  V  D  S  G  V  L  P  S  Y
1541   TTCAGTAATGTGACAGCAGTTCTGCAGCAGCAGgtaaactcacaaacactttgattt//t  2500
         F  S  N  V  T  A  V  L  Q  Q  Q
2501   gaggggggcggatctctctgtgtctcactcagGACAGCGCATCCTGTGGTTGGATGTCTCT  2560
                                        D  S  A  S  C  G  W  M  S
2561   GAAGAGAGATCTGCTCCGGGTCCTAGAGTCCACCCTTCACCATCAGCCCTCTTGTTTCAC  2620
       L  K  R  D  L  L  R  V  L  E  S  T  L  H  H  Q  P  S  C  F
2621   CTGGAGACATGCCCACTGA                                          2639
       T  W  R  H  A  H  S
```

C. IFNd

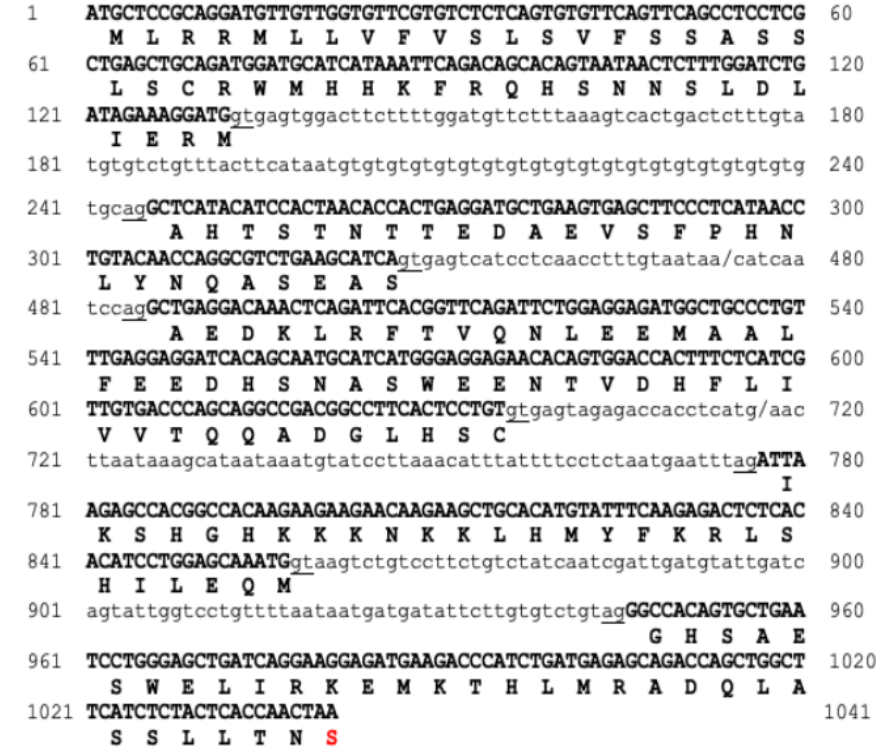

Figur 4.2 Nucleotide and deduced amino acid (aa) sequence of lumpfish A. *IFNh*, B. *IFNc* and C. *IFNd*. The putative aa sequence is shown under the third aa of the triplet codon and stop condons are in red. Parts of introns are left out of the figure (indicated by slash).

A characteristic feature of type I *IFN* genes is the unique genomic organization consisting of five exons and four introns in phase 0 (Zou, 2011), which was also found to be true for lumpfish *IFNs* (Fig. 4.3). For lumpfish *IFNd*, all exons except exon four were of the same size as the corresponding in *IFNd* of stickleback. Interestingly, exon two, three and four of lumpfish *IFNh* were of the same length as the corresponding in stickleback.

The two conserved cysteines in all three lumpfish type I IFNs were located in exon one and three, predicted to form an intracellular disulfide bond (cys1-cys3) in the mature peptides. The two additional conserved cysteines in type I group II IFNs, predicted to form an additional intracellular disulfide bond, were located in exon two and four (Cys2-Cys4) (Fig. 4.3).

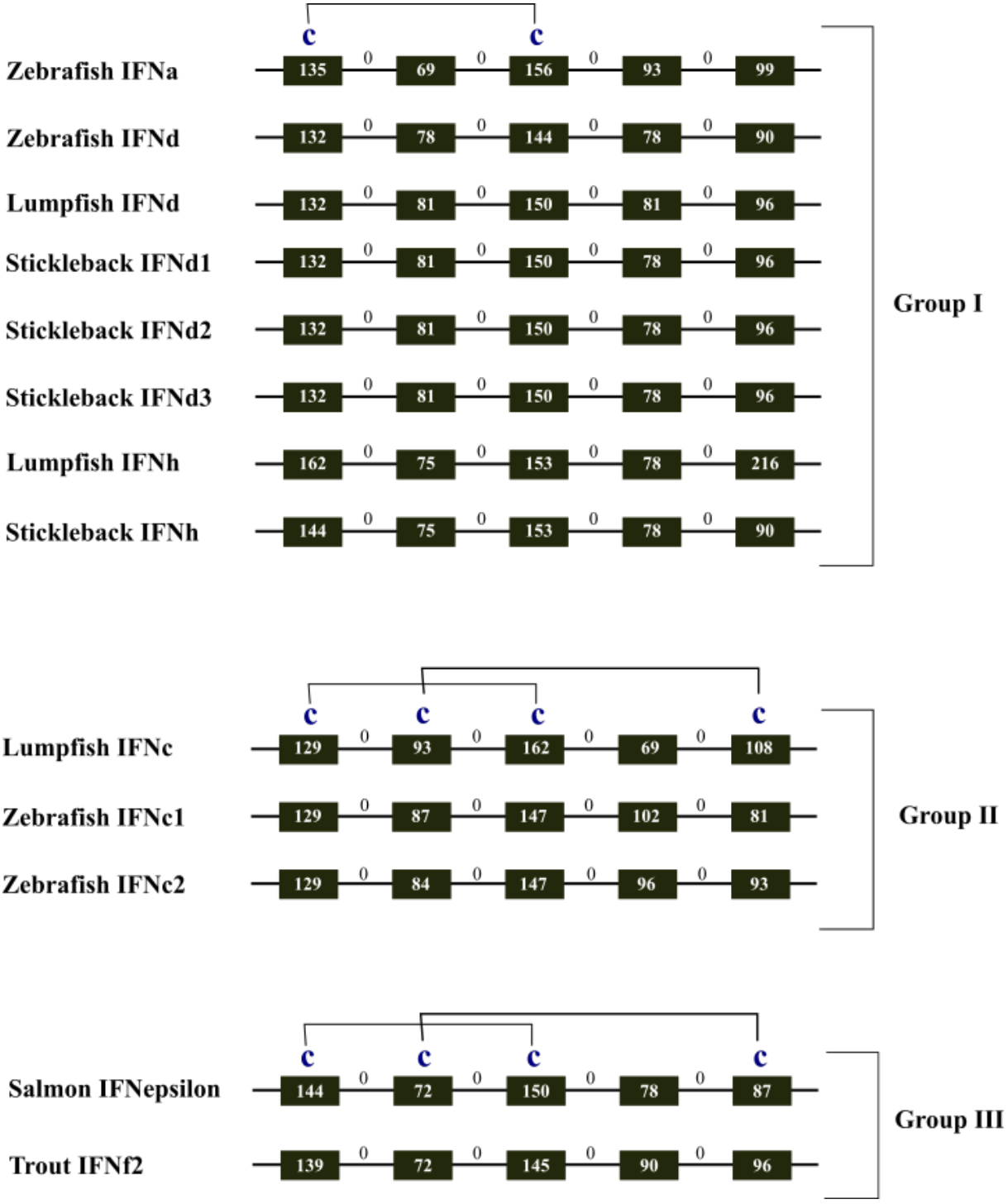

Figure 4.3 Genomic organization of *IFN* genes in lumpfish, zebrafish and stickleback. The black boxes represent exons while the line between the boxes represent introns. The exon size in bp is numbered in the box and the intron phase is indicated above the introns. Conserved cysteines are indicated in blue and predicted intracellular disulphide bonds are represented as lines between the cysteines.

To investigate if the lumpfish *IFN* genomic localization was conserved, synteny was performed and comparatively analyzed with zebrafish and stickleback revealing conserved synteny in the region encoding *IFNs* (Fig. 4.4). Two *IFN* clusters were found for lumpfish, located on chromosome 5 and 19. On chromosome 5, *ARHGAP27l* was found upstream of *IFNh* and *IFNc*, and *GH1* and *SCN4AA* downstream. The synteny was retained for zebrafish and stickleback, except for *SCN4AA* not being found in stickleback. On chromosome 19, two *IFNd* genes were identified, named *IFNd1* and *IFNd2*. *PLEKHM1* were found upstream of *IFNd1* and *IFNd2*, and *CD79B, SCN4AA* and *ARGAP27L* were downstream. This synteny was also retained for stickleback and zebrafish, except for *ARHGAP27L* being located upstream of their *IFNd.* Additionally, the synteny revealed lumpfish to have two *IFNd* isoforms, named *IFNd1* and *IFNd2*.

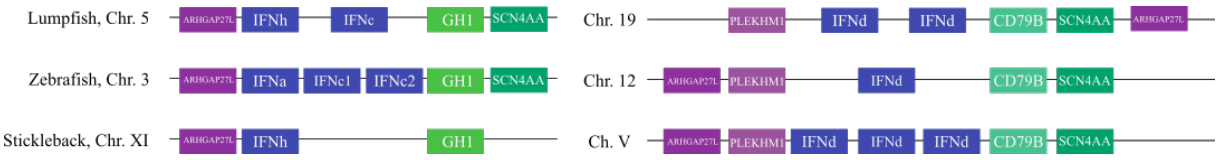

Figure 4.4 Comparative synteny analysis of type I *IFN* genes in lumpfish, zebrafish and stickleback was predicted using Genomicus, NCBI and Figure 2 (Liu et al, 2019). Two homologous *IFN* loci was found for all three fish investigated, one linked to *GH1* and one linked to *CD79B*.

4.4 Peptide analysis and phylogenetic relationship of lumpfish type I IFNs

Peptide analysis revealed the putative proteins of IFNh, IFNc and IFNd to consist of 215 aa, 186 aa and 179 aa, respectively (Fig. 4.2). A signal peptide was predicted from Met^{1} to Leu^{26} in the IFNh putative protein, Met^{1} to Val^{21} in the IFNc putative protein and Met^{1} to Leu^{20} in the IFNd putative protein (Fig. 4.2).

Multiple sequence alignment (MSA) of IFN peptide sequence with both distant and closely related teleost species (Fig. 4.5) in addition to an InterProScan analysis confirmed the lumpfish IFN candidates to be type I IFNs, containing a four helical bundle. All teleost IFNs investigated retained at least two conserved cysteines and six α-helices (named A-F), which is a well-known characteristic of type I IFNs (Hamming et al., 2011). The first conserved cysteine is almost immediately after the signal peptide, while the other is

approximately 120 aa through the sequence. Type I Group II IFNs have 4 conserved cysteines, with the 3rd approximately 25 amino acids after the 1st conserved cysteine and the 4th about 30 amino acids from the C-terminus. These findings correlate with IFNh and IFNd being type I group I IFNs containing two conserved cysteines and IFNc being a type I group II IFN with four conserved cysteines.

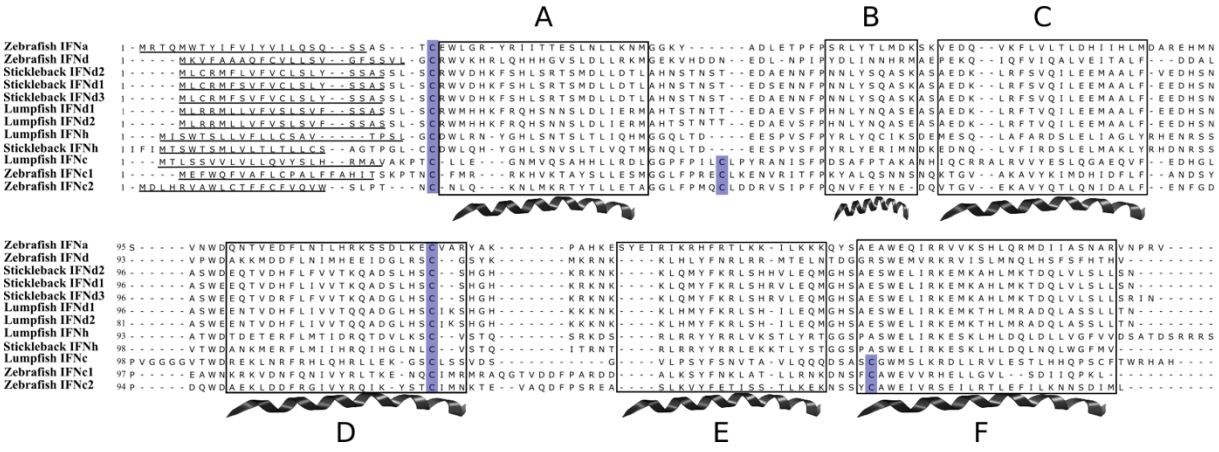

Figure 4.5 Multiple sequence alignment of lumpfish type I candidates along with, zebrafish and stickleback type I IFNs. The MSA was generated with Muscle using the Ugene software. α-helices predicted from superimposed crystographic structured of zebrafish IFNa are indicated by black boxes (Hamming et al., 2011), visualized with inkscape. Predicted signal peptides are shown by black line.

To analyze the evolutionary relationship of lumpfish IFNs and other known teleost type I IFNs, a phylogenetic tree was constructed with full length ORFs using neighbor-joining method (Figure 4.6). The tree clearly displayed three type I IFN groups and seven subgroups, disclosing the lumpfish putative proteins to be IFNh, IFNc and IFNd. It was clear that IFNc grouped in a major clade formed by fish IFNc sequences, which belonged to group II type I IFNs, while IFNd and IFNh were clustered with their respective orthologues belonging to group I type I IFNs. All three IFNs clustered with other species from the order Perciformes; IFNh and IFNd clustered stickleback, whilst IFNc were in a clade with meagre, turbot and flounder. Taken together, these findings confirms that two of the three known fish type I IFN groups are present in lumpfish, with expansion of group II genes into two subgroups (IFNh and IFNd1/d2). As IFNd1 and IFNd could not be distinguished on peptide nor nucleotide level, IFNd further used in this study refers to both IFNd1 and IFNd2.

Figure 4.6 Phylogenetic tree analysis of teleost type I IFNs. The phylogenetic tree was generated by the Neighbour-Joining method with the MegaX program, using MSA of full length protein sequences. The JT matrix-based method with pairwise deletion option was chosen to compute the evolutionary distance. The percentage bootstrap value is shown as percentage based on 1000 replicates. The lumpfish IFN are indicated by bold font.

5.5 Lumpfish IFNs structure prediction

Structure prediction of lumpfish IFNs was performed with swiss-model homology modelling, searching for homologous sequences as templates and building models based on target-template alignment using ProMod3. Conserved coordinates were copied from template to model, whilst insertions and deletions are remodeled using a fragment library (Bertoni et al., 2017, Bienert et al., 2017, Waterhouse et al., 2018, Studer et al., 2020, Studer et al., 2021). IFNh was built with human interferon-receptor complex (PDB entry 2kz1) as template, IFNc with zebrafish interferon 2 (PDB entry 2PIw) and IFNd with zebrafish interferon 1 (PDB entry 3PIV). All three predicted structures were visualized with Pymol (Fig. 4.7).

All three predicted structures revealed a typical type I IFN architecture containing six conserved alpha helices designated A-F, with helix B being the most narrow and variable (Fig. 4.7). The core was made up of helices A, C, D and F, defining the structural core of class II helical cytokines. Both IFNh, IFNc and IFNd exhibited a straight F helix, characteristic for type I IFNs giving them an elongated elliptical shape. For IFNh and IFNd contained two conserved cysteines, one disulfide bridge was present linking the N-terminus to Helix d, whilst IFNc contained two additional cysteines and thus an additional cysteine bridge linking the AB loop to helix F (Hamming et al., 2011).

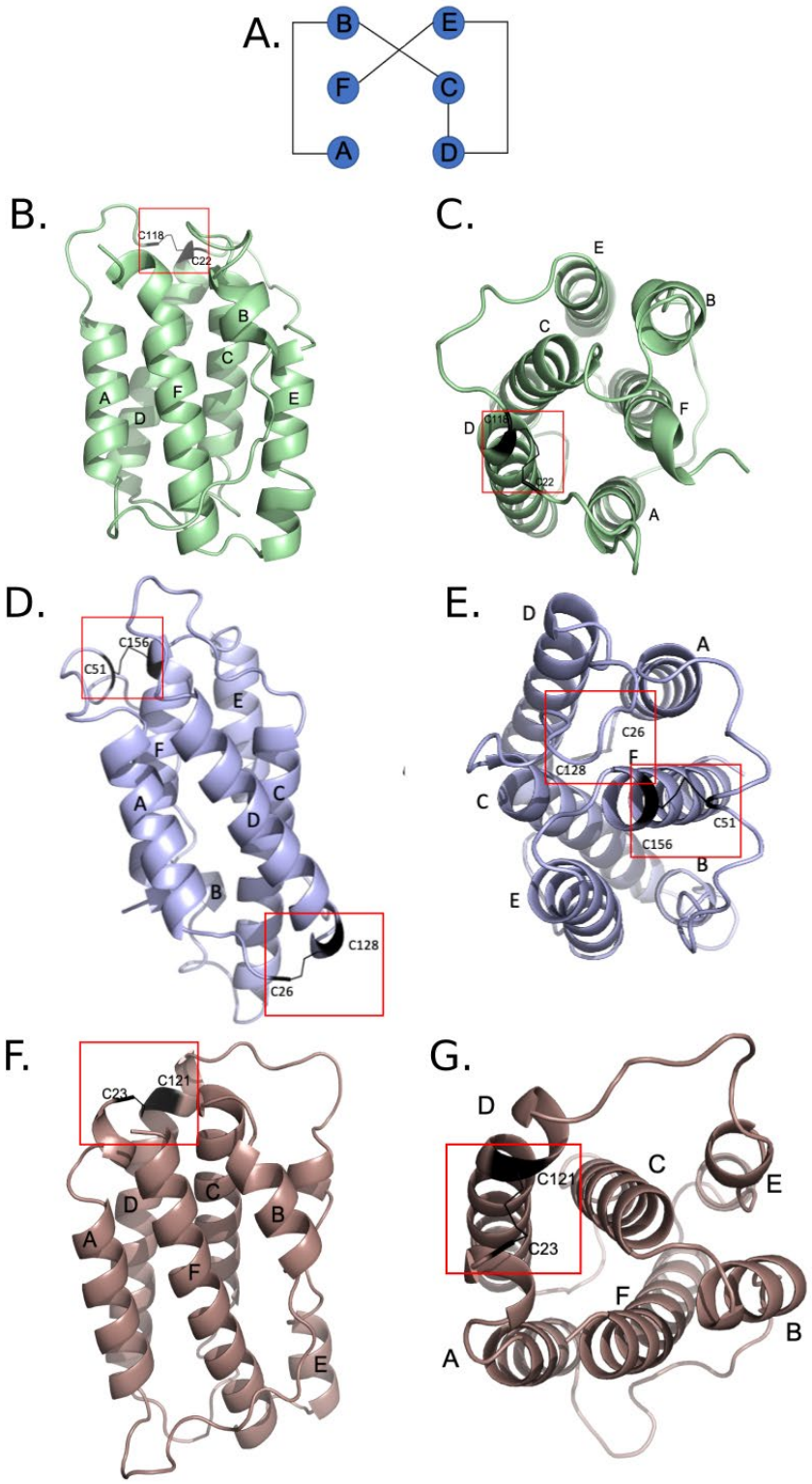

Figure 4.7 Predicted structures of lumpfish IFNh, IFNc and IFNd. A. Schematic representation of the secondary structure elements (named A-F) of type I IFNs. **B. & C.** Side and top view of predicted IFNh structure. Conserved cysteines are colored black and predicted disulfide bridges are indicated by red boxes. **D. & E.** Side and top view of predicted IFNc structure. Conserved cysteines are colored black and predicted disulfide bridges are indicated by red boxes. **F. & G.** Side and top view of predicted IFNd structure. Conserved cysteines are colored black and predicted disulfide bridges are indicated by red boxes.

4.6 Validation of PCR-assays used to quantify IFN *transcripts*

To quantify *IFNh, IFNc* and *IFNd* RNA basal levels in nine tissues, in addition to expression levels after *in vitro* and *in vivo* stimulation with PAMPs, qPCR was performed. The efficiency of the assay are given in table 4.3 and validation of the assay is shown in Fig. 5.8. The qPCR products were present as bands between 100 and 50 bp, which corresponds with the expected size of the *IFNh*, *IFNc* and *IFNd* products to be 64 bp, 94 bp, and 80 bp, respectively. cDNA without RT in addition to NTC (no template) served as negative controls, in which no bands were detected (Fig 4.8).

Table 4.3 qPCR assay

Target	y	R2	E	Size (bp)
IFNh	-3,26	1.00	2.03	64
IFNc	-3.26	1.00	2.03	94
IFNd	-3.79	0.97	1.84	80

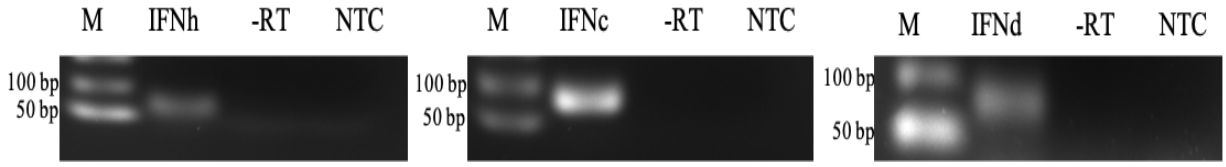

Figure 4.8 Validation of PCR assays used to quantify *IFN*s in lumpfish. The PCR product of *IFNh*, *IFNc* and *IFNd* served as positive controls, while cDNA without RT in addition to NTC (no template) served as negative controls.

4.7 Tissue-specific expression of lumpfish IFN *genes*

To functionally analyze IFNs in lumpfish, the expression patterns of *IFNh, IFNc* and *IFNd* in different tissues of healthy fish was assessed by real-time qPCR using *RSP20* as reference gene (Fig. 4.9). The constitutive expression levels in muscle, spleen, gill, liver thymus, midgut, hindgut and skin were analyzed, revealing very low expression in all tissues except midgut. Constitutive expression of *IFNc* and *IFNd* was highest in midgut followed by skin and hindgut. In contrast, constitutive expression of *IFNh* was only detected in midgut. When comparing *IFNh, IFNc* and *IFNd* expression within the same tissue, it was clear that *IFNh* was significantly lower than the others. IFNc was highest in all tissues where *IFN* expression was detected except for hindgut where *IFNd* was the highest. When comparing each tissue, midgut and skin appears to have the highest *IFN* expression.

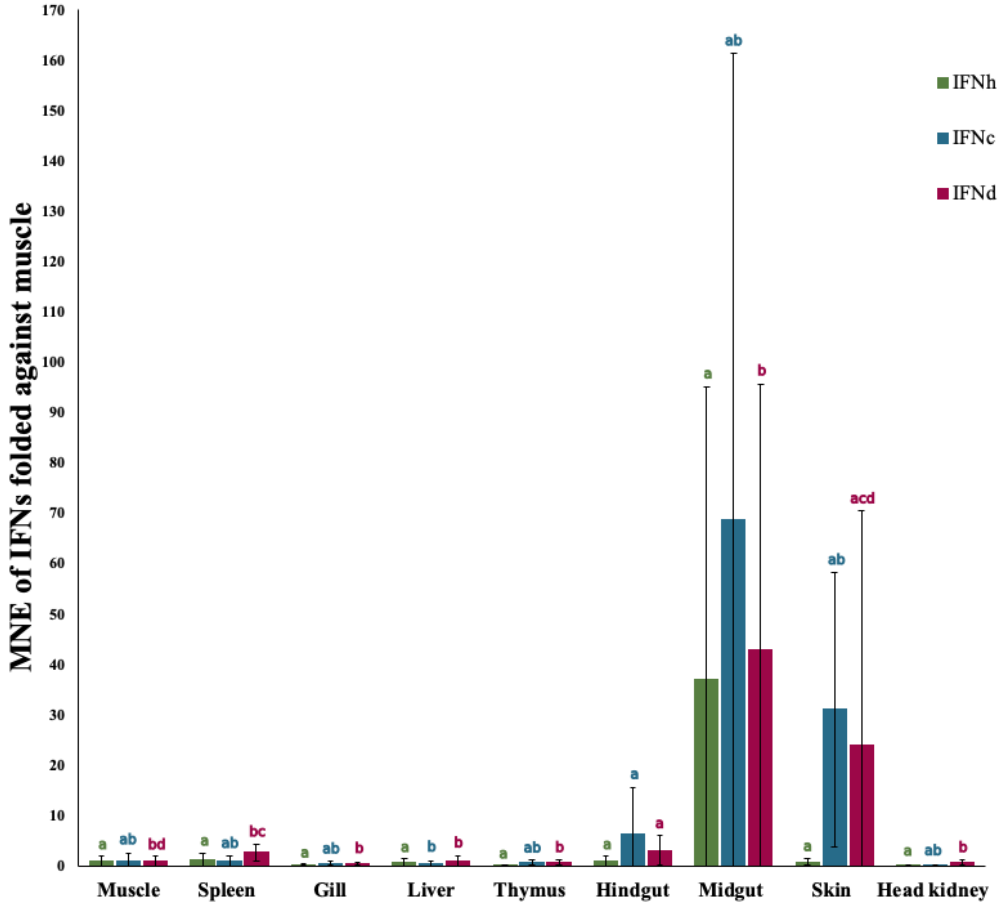

Figure 4.9 Constitutive expression of *IFNh, IFNc* and *IFNd* in muscle, spleen, gill, liver, thymus, front intestine, back intestine, skin and kidney obtained from healthy lumpfish. The expression of transcripts was normalized to the expression of the housekeeping gene *RPS20* and folded against muscle. For tissues where no gene expression was detected, the CT value was set to 40. Different letters above bars denotes a significant relationship.

4.8 In vitro immune stimulation of IFNs

To study the effect of both viral and bacterial infection on IFN expression, leukocytes isolated from HK were stimulated *in vitro* with polyI:C, R848 and *V. Anguillarum* for 4 and 24 hours. Following polyI:C stimulation, both *IFNh* and *IFNc* were significantly upregulated both 4 and 24 hpe, with the highest expression 24 hpe (Fig. 4.10). Contrarily, *IFNd* showed a very low increase in expression 4 hpe and had returned to baseline level 24 hpe. Post R848 stimulation, both *IFNh*, *IFNc* and *IFNd* exhibited baseline levels of expression 4 hpe, whilst *IFNh* and *IFNc* showed significantly increase in expression 24 hpe. A similar expression pattern was seen after *V. Anguillarum* stimulation, with the exception of *IFNd* being upregulated 4 hpe. When comparing the genes within the same stimulation group, *IFNh* exhibits the highest expression for all stimulation groups except post R848 stimulation where *IFNc* were most upregulated, while *IFNd* have the lowest if any expression for all three groups. *IL-β* serves as positive control for *V. anguillarum* as it is known to be highly upregulated when HKL is exposed to bacteria (Eggestøl et al., 2018).

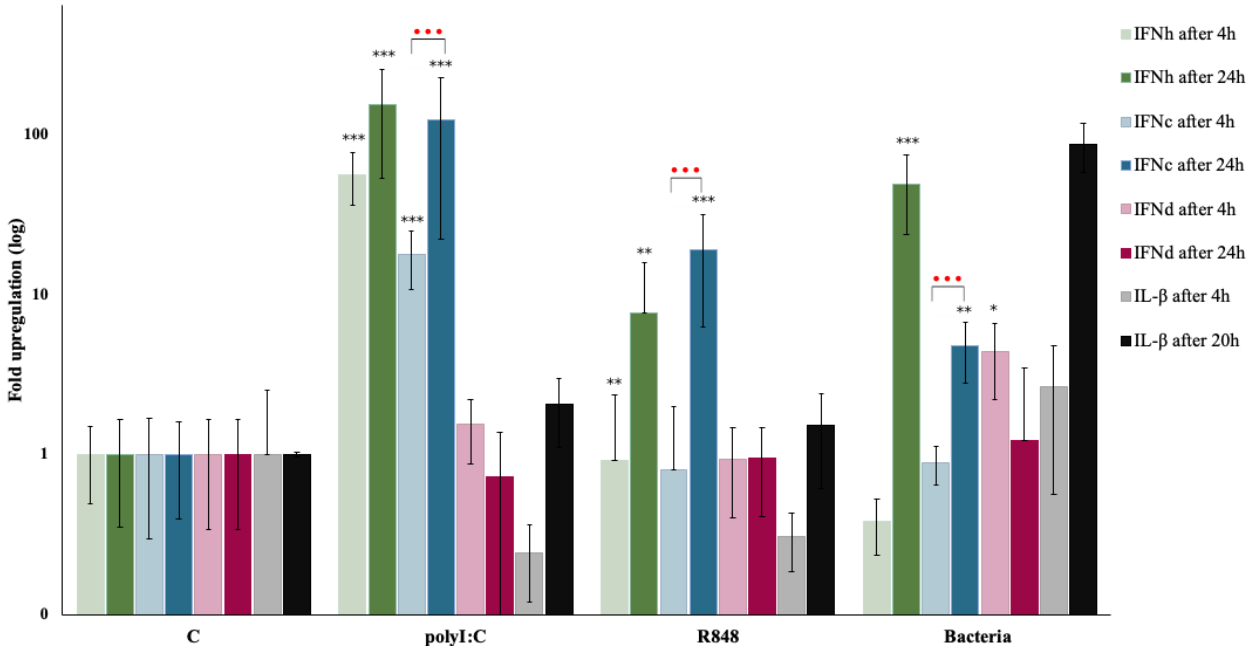

Figure 4.10 Expression of *IFNh*, *IFNc* and *IFNd* post stimulation with polyI:C, R848 and *V. anguillarum*, detected both 4 and 24 hpe of lumpfish leukocytes *in vitro*. All transcripts was normalized to the expression of the housekeeping gene *RSP20* and folded against the control. Statistically significance for each gene exposed to each stimulant is indicated with black stars and Statistically significance between each time is indicated by red dots (•••). $p<0.001$ = ***, $0.001<p<0.01$ = ** and $p<0.05$ = *.

4.9 In vivo *immune stimulation of IFNs*

To study the impact of virus infection of IFN expression *in vivo*, healthy lumpfish was injected with polyI:C before spleen and HK was dissected out 6 and 24 hours post injection (hpi).

In both HK and spleen, *IFNh* exhibited the highest expression profile 6 hpi, whilst *IFNc* were more expressed 24 hpi (Fig. 4.11). Low expression was seen for *IFNd* in both tissues. When comparing genes within the same tissue, *IFNc* and *IFNh* had the highest expression level in spleen, whilst *IFNd* was significantly lower. A similar expression pattern was seen for HK, with little difference between *IFNh* and *IFNc* expression.

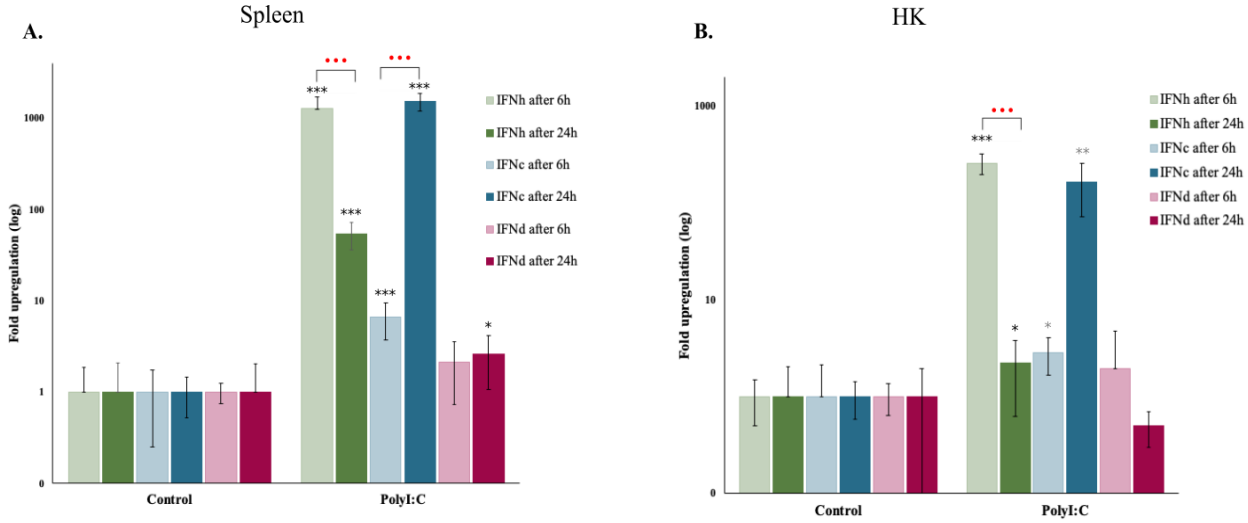

Figure 4.11 Expression of *IFNh, IFNc* and *IFNd* after *in vivo* stimulation of lumpfish with polyI:C. A. *IFN* expression in spleen 6 and 24 hpi with polyI:C in lumpfish. **B.** *IFN* expression in HK 6 and 24 hpi with polyI:C in lumpfish. Statistically significance of each tissue gene is indicated with black stars for P value < 0.05 and grey stars for P value > 0.05. Statistically significance between each time is indicated by red dots (•••). p<0.001 = ***, 0.001<p<0.01 = ** and p<0.05 = *.

4.10 Recombinant IFN expression and purification

The *in vitro* and *in vivo* stimulation experiments clearly indicated that IFNh and IFNc are involved in antiviral defense. To investigate whether the two IFNs were able to activate the type I IFN signaling pathway and induce Mx expression, they were cloned into pET21a in frame with a C-terminal his-tag. The sequences were confirmed with sanger sequencing. Recombinant IFNh and c were expressed in two strains of *E. coli*, BL21 (DE3) and codon plus. Three colonies of each IFNh and IFNc were expressed in both strains, seen as bands with the predicted molecular weight at approximately 21 and 25 kDa, respectively (Fig. 4.12). The expression of the IFNs is shown in BL21(DE3) only, but the expression level in condon plus was similar. The IFN expressing cells were lysed through French press and sonication prior to centrifugation. As seen in Fig. 4.12 the proteins were not present in the supernatant of the CE, implicating them to be inclusion bodies in the pellet. However, as minor amounts of recombinant proteins could still be in the present, the supernatant was purified with Ni^{2+}-resin (IMAC). Unfortunately, no recombinant proteins bound (data not shown) and we were not able to purify the proteins. Attempts to obtain solubilized proteins were tried using urea in the buffer, but the recombinant proteins were still present as inclusion bodies.

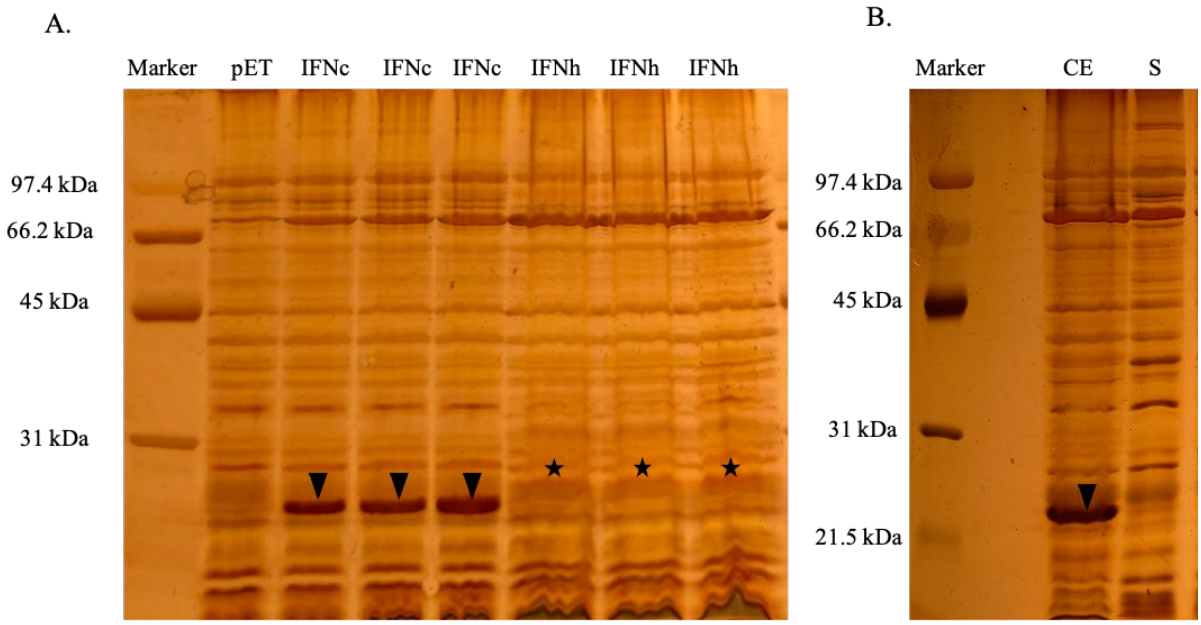

Figure 4.12 Recombinant IFN expression and purification analyzed by SDS-PAGE. **A.** IFNc (arrowhead) and h (star) expression induced by autoinduction in BL21(DE3) cells. **B.** Cell extract (CE) of BL21(DE3) cells expressing IFNc (arrowhead) and the soluble (S) fraction of CE. Arrow heads indicate the IFNc, while star represents IFNh.

5. DISCUSSION

Lumpfish is a relatively new species produced by the aquaculture industry, suffering from high mortality due to both bacterial and viral infections. Aquatic vertebrates are generally more exposed to pathogens than mammals due to the environment they occupy, and it is known that the innate immunity in teleosts are of major importance as their adaptive immune system is less developed (Haugland et al., 2012). Identification and in-depth knowledge of key molecules involved in antiviral immunity provides a valuable tool to study effect of immune modulations such as vaccination, and host-pathogen interactions. Knowledge of the innate immune responses and antiviral defense in lumpfish is additionally needed as basis for design of efficient immunoprophylactic measures to ensure further use of lumpfish in the Atlantic salmon farming industry.

IFNs are secreted cytokines able to induce transcription of ISGs and therefore vital for antiviral defense. IFN-activity was first reported in teleosts in 1965 but was not cloned until 2003 (Robertsen et al., 2003). Since then, IFNs have been reported in several fish species including salmon, trout, cod, zebrafish, yellow croaker, Japanese flounder and stickleback (Robertsen et al., 2003, Zou and Secombes, 2011). Thus far, type I IFNs have not been reported in lumpfish, therefore the aim of this thesis was to molecular and functionally characterize lumpfish IFN candidates and to sub classify them. Furthermore, transcriptome-wide analyses of the RLR signaling pathway was performed as it is known that RLRs are involved in antiviral responses (Liang and Su, 2021).

Upon viral infection, the innate immune system is activated through PRRs, which recognizes conserved pathogen motifs, triggering intracellular pathways resulting in IFN production (Aoki et al., 2013). To investigate early immune responses upon viral infection, the RLR signaling pathway was characterized by generating a KEGG pathway from DEG analysis of HKLs 6 and 24 hpe to polyI:C. Most components of the pathway were found in lumpfish, including MDA5, LGP2, MITA, IRF3, TANK, TAK1, TRIM25, CYLD, atg12, DAK, TRAF2, p38, JNK, DUBA, TRAF3, NAP1, CASP8, IKKγ, DDX3X, PIN1, IKKα, IKKβ, IκB, IL-8, IL-12, NF-κB and TRAF6 (Fig. 4.1). RIG-I and IFNs were however not identified amongst the automated annotated transcripts. LGP2, MITA, MDA5 and IRF3 were found to be most upregulated, whilst TAK1, DDX3X and IKKβ were most downregulated at 24 hpe. Consistent with these results are findings in seabream where

MDA5, LGP2, MITA and IRF3 were found to be upregulated post polyI:C stimulation (Valero et al., 2015). Similarly, a study by Ding *et al*. found that IRF3 expression is involved in IFNh expression in large yellow croaker (Ding et al., 2016). Altogether, these findings indicate that upon MDA5 activation by polyI:C, IFN expression is induced through MITA and IRF3 in lumpfish, with LGP2 as a potential positive regulator if MDA5. This corresponds with the fact that dsRNA induces IFN transcription through MDA5 in both fish and mammals (Gitlin et al., 2006, Zhou et al., 2014).

Interestingly, RIG-I was not identified in lumpfish, despite in-depth search in both RNA seq data. However, as RIG-I has not yet been identified in Perciformes species (Zou et al., 2009, Chen et al., 2017), it was not unexpected that it was absent in the lumpfish genome. Contrarily, we expected to find IFNs as they are pivotal for ISG induction and thus transcription of antiviral genes. As the KEGG pathway is based on the human RLR signaling pathway, lumpfish IFNs may not appear as they are not true homologs of human IFNs, we therefor continued searching for IFN candidates.

5.1 Identification of IFNh, c and d in lumpfish

IFNs in mammals can be classified into type I, II and III, with group III apparently lost in teleosts. Type I IFNs is involved in antiviral defense in teleost as in mammals, and while mammalian type I IFNs include IFNα and IFNβ, a more diversified repertoire is seen in teleosts. Based on conserved cysteines, teleost type I IFNs can be further sub-classified into three groups: the two cysteine containing group I (IFNa, d, h and e) and the four cysteine containing groups II (IFNb and c) and III (IFNf) (Huang et al., 2019). Group I IFNs exists in all teleost species investigated, whilst group II and III are limited to certain species. The diversified repertoire of IFNs in fish compared to mammals can be explained by the fact that teleosts have had a second round (2R) of whole-genome duplication (WGD) during their early evolution (Liu et al., 2020), and some species (belonging to the orders Salmoniformed and Cypriniformes) have even has a third round of WGD (Glasauer and Neuhauss, 2014).

After further searching the RNA ref seq data, three lumpfish IFN candidates were identified and classified as type I IFNs due to their predicted four helical core. This was further substantiated when sequence analysis was performed, exhibiting conserved

exon/intro and genomic organization (Fig. 4.2 and 4.3). Upon performing a MSA with known IFN sequences of both distant and closely related fish species, a conserved cysteine pattern was seen further subclassifying them to group I and II (Fig. 4.5). tBLASTp search and phylogenetic analysis designated the candidates IFNh, IFNc and IFNd due to sequence similarity with their respective IFNs of other species (Fig. 4.6). These findings correlated with earlier studies stating species in the class Perciformes possess these three subgroups with IFNh appearing to be specific for species such as meagre, yellow croaker, Japanese flounder and Nile tilapia (Milne et al., 2018, Ding et al., 2017, Hu et al., 2017, Gan et al., 2020), belonging to the superorder Acantopthergyii.

As previously stated, multiple copies of IFNs are common due to their second round of WGD. However, teleost gene synteny is well conserved with two *IFN* loci, linked to either *GH1* or *CD79B* (Liu et al., 2019). In lumpfish *IFNc* and *IFNh* were grouped together with *ARHGAP27L* upstream and *GH1* and *SCN4AA* downstream, whilst two *IFNd* genes were found clustered together with *PLEKHM1* upstream and *CD79B, SCN4AA* and *ARHGAP27L* downstream (Fig. 4.4). This gene synteny was also found to be retained in Stickleback, zebrafish and spotted gar (Liu et al., 2019). Studies have suggested the *IFN* loci to be unstable, thus contributing to IFN diversity through insertions and deletions of IFNs (Liu et al., 2019). Interestingly, the lumpfish gene synteny revealed presence of two *IFNd* genes flanking each other. Further sequence analysis indicated them to have arisen by gene duplication, as they could not be distinguished on nucleotide level and thus not by qPCR.

5.2 Teleost IFNs exhibit a conserved genomic organization

When analyzing the phylogenetic relationship of teleost IFNs, the phylogenetic tree clearly displayed type I IFNs to be grouped into three groups (Fig. 4.4), which have been heavily debated. It has been postulated that type I IFNs is only arranged into group I and II due to phylogenetic analysis and IFNf containing four conserved cysteines, thus being a group II IFN (Zou et al., 2021). However, in other phylogenetic analysis, including in this study, IFNf of several species were arranged into their own group. This is substantiated by a high bootstrap value (98%) of group III in Fig. 4.6. The inconsistent grouping of IFNs could be explained by different methods and bootstraps values for three generations, indicating that further sequence and phylogenetic analysis should be performed to enable a conclusion.

However, IFNf is hypothesized to be an ancient IFN isoform of Gnathostome vertebrates, thus grouping into its own clade in the phylogenetic tree (Liu et al., 2019).

5.3 Type I IFNs contains a conserved four helical bundle

It has been heavily debated on whether type I IFNs of teleosts are homologous to type III or type I IFNs in mammals. Fish type I IFN genes share the same genomic organization with mammalian type III genes with five exons separated by four phase zero intron. However, in 2011 crystal structures of zebrafish IFNs were resolved (Hamming et al., 2011), exhibiting a characteristic helical structure resembling human type I IFNs (Zou et al., 2021). This was also found in this study when predicting the structure of lumpfish IFNs based on homology modelling (Fig. 4.7). All three IFNs contained six conserved α helices named A-F, with A, C, D and F contributing to the helical core. Helix F also exhibited a straight elongated shape, contributing to the overall shape resembling an American football (Hamming et al., 2011). IFNc and IFNd was built with zebrafish IFNs as template, whilst IFNh had human type I IFN-receptor complex as template, further substantiating fish type I IFNs being homologous to mammalian type I IFNs. The two conserved cysteines of all three sequences contributed to disulfide bridges linking the N-terminus to helix D, while the two additional cysteines in IFNc linked the AB loop to helix F. These disulfide bridges have been found to be essential for both protein conformation and biological activity (Beilharz et al., 1986). Earlier studies have shown that mutation in the conserved cysteines affected the bioactivity leading to reduction in its antiviral activity (Beilharz et al., 1986, Shepard et al., 1981).

Taken together, we can conclude that lumpfish have three IFNs belonging to type I group I (IFNh) and group II (IFNc and IFNd) IFNs, with all three exhibiting a conserved genomic organization. As IFNd1 and IFNd2 could not be distinguished on nucleotide level, only one IFNd is used and described further in this study.

5.4 Type I IFN*s exhibit a constitutively, low expression in healthy individuals*

Generally, teleost type I IFNs are constitutively expressed at low levels in healthy individuals, with group I ubiquitously expressed at a higher level than group II IFNs. This may indicate that group I IFNs act as the first wave of IFNs post viral infections, possibly

enhancing transcription of group II IFNs (Zou et al., 2021). Contrarily, this study found the group II *IFNc* to exhibit the highest expression in both midgut, hindgut and spleen of lumpfish (Fig. 4.9). *IFNh* (group I) was only detected in midgut, whilst *IFNd* expression was found at low levels in spleen, hindgut, midgut and skin. Similar results were seen in both mandarin fish and meagre, where *IFNc* exhibited the highest expression in most tissues, whilst *IFNh* and *IFNd* were significantly lower expressed (Milne et al., 2018, Langhari et al., 2018). This may suggest a diversified IFN expression pattern amongst teleost, with apparently some consistency amongst species in the order Perciformes. This could be explained by Perciformes species possessing the same IFNs; IFNh, IFNc and IFNd. Interestingly, when comparing tissues, the highest *IFN* expression was found in midgut and skin, which corresponds with their role as primary barriers of invading pathogens. However, in this study, *IFN* expression was not detected in most tissues investigated in addition to most of the results not being statistically significant. It is therefore evident that experiment should be repeated, and no conclusions about basal expression of IFNs in lumpfish can be conducted.

5.5 PolyI:C, R848 and bacteria induce upregulations of IFNs in vitro

To investigate the impact of virus and bacteria on IFN expression, an *in vitro* stimulation experiment was performed. Lumpfish HKLs were exposed to PAMPs; polyI:C (synthetic dsRNA), R848 (synthetic ssRNA) and whole bacteria (*V. anguillarum*). Post polyI:C stimulation *IFNh* was most upregulated both 4 and 24 hpe, followed by *IFNc*, whilst *IFNd* was not significantly regulated in lumpfish (Fig. 4.10). Corresponding results were also seen in a study by Milne *et al.* where meagre HKLs were exposed to polyI:C, resulting in *IFNh* being most upregulated, followed by *IFNc* and *IFNd*, respectively (Milne et al., 2018). Stimulation with R848 in this study, indicated *IFNh* and *IFNc* not to be regulated 4 hpe, but with a significant upregulation of *IFNc* followed by *IFNh* 24 hpe. *IFNd* exhibited baseline levels of expression at both 24 and 4 hpe. Similarly, mandarin fish HKLs exposed to R848 resulted in significant upregulation of *IFNh* and *IFNc*, while *IFNd* was hardly upregulated at all (Langhari et al., 2018). In our data, both *IFNh* and *IFNc* expression had high statistical significance post PAMP stimulation, while only the time difference in IFNc showed statistical significance. The data from *IFNd* expression was not significant, which could be explained by the very low expression levels.

When comparing *IFN* expression post stimulation with polyI:C and R848 it is evident that polyI:C induces a higher and more rapid upregulation of *IFNh* and *IFNc*, compared to R848. This can be explained by polyI:C (dsRNA) inducing IFN expression through TLR3/MDA, while R848 (ssRNA) induces IFN expression through TLR7/8. This is also consistent with the KEGG analysis, as MDA5 was upregulated post exposure to polyI:C (Fig. 5.1).

5.6 In vivo *stimulation with polyI:C provokes upregulation of* IFNh *and* IFNc

The expression levels of IFNs post polyI:C exposure was also investigated in an *in vivo* stimulation experiment. Samples from spleen and HK were taken out 6 and 24 hours post injection (hpi) of polyI:C. Interestingly, *IFNh* was the most upregulated 6 hpi and *IFNc* was most upregulated 24 hpi, in both tissues investigated (Fig. 4.11). *IFNd* was not significantly regulated. These data resemble the results from the *in vitro* experiment, where *IFNh* and *IFNc* was found to be the most upregulated, with the exception of both genes being most upregulated after 24h. However, the rapid induction of the group I *IFNh*, compared to the group II *IFNc*, further imply their transcription to be induced through different pathways. Previous studies in salmon have demonstrated that group I IFN promoters resembles mammalian IFNβ promoters, being composed of NF-κB binding site flanked by two IRF-binding sites. Group II IFNs on the other hand was found to lack NF-κB binding site, thus being activated through TLR7/8 pathways (Huang et al., 2019). Furthermore, studies in zebrafish demonstrated that the IFN receptor CRFB5/IFNAR1 is common for both group I and II IFNs, while CRFB1/IFNAR2-2 and CRFB2/IFNAR2-2 interacts with group I and II respectively, thus showing ligand specificity (Zou et al., 2021, Zou and Secombes, 2011). This ligand specificity could be due to the presence of two conserved cysteines in group I IFNs and four conserved cysteines in group II IFNs. These findings further substantiate IFNs in lumpfish to be activated through different PRRs and having distinct roles in inducing and maintaining an antiviral state in the host cell.

The gene expression results of the *IFNs* correlate with mandarin fish where *IFNh* were the most upregulated and *IFNd* the least (Laghari et al., 2018). However, in meagre *IFNd* was the most upregulated post polyI:C injection, followed by *IFNc* and *IFNh* (Milne et al., 2018). These inconsistent expression data is further substantiated by studies in salmon where the antiviral role of *IFNd* is not detected (Svingerud et al., 2012). Furthermore, IFNd

transgenic medaka, showed increased susceptibility to nervous necrosis virus, indicating that IFNd has a role in antiviral immunity (Maekawa et al., 2017). Due to its inconsistent role in antiviral response, it has been proposed that IFNd is involved in bacterial infections which is interesting as the highest expression of lumpfish IFNd in this study was 4 hours post bacterial stimulation *in vitro*. Similarly, in both large yellow croaker, rock bream and trout, IFNd expression was found to be significantly upregulated after exposure to bacteria (Ding et al., 2017, Chang et al., 2009, Wan et al., 2012). Contrarily, only IFNd was found to phosphorylate IRF3 and IRF7 in large yellow croaker and thus be involved in regulation of IFN expression (Ding et al., 2016). This indicates that further studies on IFNd expression should be performed in order to conclude on its role in immunity.

5.7 Expression and purification of lumpfish IFNs

The *in vitro* and *in vivo* stimulation experiments indicated IFNh and IFNc to be involved in antiviral response. If true type I IFNs, they should have the ability to induce the expression of ISGs such as Mx. Therefore, the IFNh and IFNc genes were inserted into pET21a vectors before transformed into BL21(DE3) cells and protein expression were induced. The recombinant protein was successfully expressed (Fig 4.12), but analysis of the soluble fraction of the CE revealed no presence of the proteins in the supernatant, indicating them to be insoluble. This is substantiated by human IFNs which is present as inclusion bodies in the CE (Srivastava et al., 2005). Due to the insoluble nature of the IFNs we were not able to purify them. Urea was included in the buffers, but the recombinant proteins were still insoluble. To insolubilize the inclusion bodies for future experiments, the CE pellet containing the aggregated proteins could be resuspended in a buffer with higher urea concentration, as urea break non-covalent interactions. Furthermore, a different expression system could be considered as expression of eukaryotic proteins in prokaryotic expression systems could lead to accumulation of proteins as inclusions bodies. This may be due to lack of post translational modifications in prokaryotic expression systems which some eukaryotic proteins require to correctly fold and remain soluble (Khow and Suntrarachun, 2012). Teleost IFNs are known to have glycosylation sites, indicating that post-translation glycosylation is critical for correct structure and stability (Pereiro et al., 2014, Huang et al., 2015, Wu et al., 2018).

6.8 Conclusion

In-depth knowledge about key molecules involved in antiviral defense is therefore needed, both to study the effect of immune modulations and host-pathogenic interactions, but also as basis for design of vaccines. Therefore, this study aimed to identify early immune responses and to characterize IFNs in lumpfish.

Most components of the RIG-I pathway was identified, with LGP2, MDA5, MITA and IRF3 being most upregulated post exposure to polyI:C. Furthermore, three IFN candidates were identified in RNA ref seq data, determined to be IFNh, IFNc and IFNd through bioinformatical analysis, which correlated with other perciform species. Sequence, protein structure models, synteny and genomic organization revealed conserved organization, confirming them to be type I IFNs. The presence of two conserved cysteines in IFNh and d and four in IFNc, classified them as group I and II IFNs, respectively. Further subclassification was confirmed by phylogenetic and genomic analysis, in which lumpfish IFNs clustered with their respective IFNs of other perciform species.

All three *IFNs* were found to be constitutively expressed at a low level of health individuals in nine tissues where *IFN* expression was detected, whereas upregulation of the expression was detected post PAMP stimulation. Through both *in vitro* and *in vivo* stimulation experiments, IFNh and IFNc was found to likely be involved in antiviral defense, while IFNd may be involved in bacterial response.

These findings indicate that MDA5, IRF3, IFNh and IFNc are pivotal for antiviral defense in lumpfish and could possibly provide a basis for both development and evaluation of efficient immunoprophylactic measures.

6.9 Future perspective

This study have focused on identifying and characterizing IFNs in lumpfish, in addition to investigate the RIG-I pathway post exposure to polyI:C. Our findings displayed lumpfish to contain IFNh, c and d, with different expression profiles post PAMP stimulation assays, both *in vivo* and *in vitro*. However, further research is needed to fully understand expression and regulation of IFN post viral infections, in addition to gaining insight into the IFN signaling pathway in lumpfish.

To confirm the antiviral activity of IFNs it would be useful to infect lumpfish leukocytes with virus to see if IFNh and IFNc are able to inhibit virus replication. Additionally, it would be useful to a transcriptome-wide analysis of TLR and NLR signaling pathways upon exposure to polyI:C, to investigate other possible induction pathways of IFNs. To gain a better understanding of the induction and regulation of IFNs in lumpfish it would be beneficial to investigate the IFN promoters. Furthermore, it would be interesting to investigate the expression of the IFN receptor subunits CRFB1, CRFB1 and CRFB5 at a mRNA level post polyI:C seen in relation with IFN expression.

Gaining a better understanding of antiviral response pathways in lumpfish is crucial not only for basal knowledge of their immune system, but also as basis for design of efficient immunoprophylactic measures. As lumpfish suffers from high mortality, effective medicine and vaccines are crucial for continuing using the fish as a delousing measure in the Atlantic salmon farming industry.

7. REFERENCES

AKIRA, S., UEMATSU, S. & TAKEUCHI, O. 2006. **Pathogen recognition and innate immunity**. *Cell,* 124**,** 783-801.

ALTMANN, S. M., MELLON, M. T., DISTEL, D. L. & KIM, C. H. 2003. **Molecular and functional analysis of an interferon gene from the zebrafish, *Danio rerio***. *J Virol,* 77**,** 1992-2002.

AOKI, T., HIKIMA, J., HWANG, S. D. & JUNG, T. S. 2013. **Innate immunity of finfish: primordial conservation and function of viral RNA sensors in teleosts**. *Fish Shellfish Immunol,* 35**,** 1689-702.

BAOPRASERTKUL, P., XU, P., PEATMAN, E., KUCUKTAS, H. & LIU, Z. 2007. **Divergent Toll-like receptors in catfish (*Ictalurus punctatus*): TLR5S, TLR20, TLR21**. *Fish Shellfish Immunol,* 23**,** 1218-30.

BEILHARZ, M. W., NISBET, I. T., TYMMS, M. J., HERTZOG, P. J. & LINNANE, A. W. 1986. **Antiviral and antiproliferative activities of interferon-alpha 1: the role of cysteine residues.** *J Interferon Res,* 6**,** 677-85.

BERTONI, M., KIEFER, F., BIASINI, M., BORDOLI, L. & SCHWEDE, T. 2017. **Modeling protein quaternary structure of homo- and hetero-oligomers beyond binary interactions by homology**. *Sci Rep,* 7**,** 10480.

BIENERT, S., WATERHOUSE, A., DE BEER, T. A., TAURIELLO, G., STUDER, G., BORDOLI, L. & SCHWEDE, T. 2017. **The SWISS-MODEL Repository-new features and functionality**. *Nucleic Acids Res,* 45**,** D313-D319.

BREILAND, M. S. W., MIKALSEN, H. & JOHANSEN, L.-H. 2014. **Susceptibility of lumpfish (*Cyclopterus lumpus*) to vibrio ordalii and infectious pancreatic necrosis virus (IPNV).** . *European Aquaculture Society Conference*

CASTRO, R. T., C 2015. **Overview of fish immunity**. *In:* PEATMAN, E. & BECK, B. H. (eds.) *Mucosal Health in Aquaculture.* Elsevier

CHANG, M., NIE, P., COLLET, B., SECOMBES, C. J. & ZOU, J. 2009. **Identification of an additional two-cysteine containing type I interferon in rainbow trout**

Oncorhynchus mykiss **provides evidence of a major gene duplication event within this gene family in teleosts.** *Immunogenetics,* 61**,** 315-25.

CHEN, S. N., ZOU, P. F. & NIE, P. 2017. **Retinoic acid-inducible gene I (RIG-I)-like receptors (RLRs) in fish: current knowledge and future perspectives**. *Immunology,* 151**,** 16-25.

CHEN, Y. M., KUO, C. E., CHEN, G. R., KAO, Y. T., ZOU, J., SECOMBES, C. J. & CHEN, T. Y. 2014. **Functional analysis of an orange-spotted grouper (*Epinephelus coioides*) interferon gene and characterisation of its expression in response to nodavirus infection**. *Dev Comp Immunol,* 46**,** 117-28.

DING, Y., AO, J., HUANG, X. & CHEN, X. 2016. **Identification of Two Subgroups of Type I IFNs in Perciforme Fish Large Yellow Croaker *Larimichthys crocea* Provides Novel Insights into Function and Regulation of Fish Type I IFNs**. *Front Immunol,* 7**,** 343.

DING, Y., GUAN, Y., AO, J. & CHEN, X. 2017. **Induction of type I interferons in response to bacterial stimuli in large yellow croaker *Larimichthys crocea***. *Fish Shellfish Immunol,* 62**,** 349-355.

DING, Y., GUAN, Y., HUANG, X., AO, J. & CHEN, X. 2019. **Characterization and function of a group II type I interferon in the perciform fish, large yellow croaker (*Larimichthys crocea*)**. *Fish Shellfish Immunol,* 86**,** 152-159.

EGGESTØL, H. O., LUNDE, H. S., KNUTSEN, T. M. & HAUGLAND, G. T. 2020. **Interleukin-1 Ligands and Receptors in Lumpfish (*Cyclopterus lumpus L.):* Molecular Characterization, Phylogeny, Gene Expression, and Transcriptome Analyses.** *Front Immunol,* 11**,** 502.

EGGESTØL, H. O., LUNDE, H. S., RØNNESETH, A., FREDMAN, D., PETERSEN, K., MISHRA, C. K., FURMANEK, T., COLQUHOUN, D. J., WERGELAND, H. I. & HAUGLAND, G. T. 2018. **Transcriptome-wide mapping of signaling pathways and early immune responses in lumpfish leukocytes upon in vitro bacterial exposure**. *Sci Rep,* 8**,** 5261.

GAN, Z., CHENG, J., CHEN, S., LAGHARI, Z. A., HOU, J., XIA, L., LU, Y. & NIE, P. 2020. **Functional characterization of a group II interferon, IFNc in the perciform fish, Nile tilapia (*Oreochromis niloticus*).** *Fish Shellfish Immunol,* 105**,** 86-94.

GAN, Z. C., N.S. HUANG, B. NIE, P. 2019. **Fish type I and type II interferons: composition, receptor usage, production and function**. *Reviews in Aquaculture,* 12**,** 773-804.

GITLIN, L., BARCHET, W., GILFILLAN, S., CELLA, M., BEUTLER, B., FLAVELL, R. A., DIAMOND, M. S. & COLONNA, M. 2006. **Essential role of mda-5 in type I IFN responses to polyriboinosinic:polyribocytidylic acid and encephalomyocarditis picornavirus.** *Proc Natl Acad Sci U S A,* 103**,** 8459-64.

GLASAUER, S. M. & NEUHAUSS, S. C. 2014. **Whole-genome duplication in teleost fishes and its evolutionary consequences.** *Mol Genet Genomics,* 289**,** 1045-60.

GUETHMUNDSDOTTIR, S., VENDRAMIN, N., CUENCA, A., SIGURETHARDOTTIR, H., KRISTMUNDSSON, A., IBURG, T. M. & OLESEN, N. J. 2019. **Outbreak of viral haemorrhagic septicaemia (VHS) in lumpfish (*Cyclopterus lumpus*) in Iceland caused by VHS virus genotype IV**. *J Fish Dis,* 42**,** 47-62.

HAMMING, O. J., LUTFALLA, G., LEVRAUD, J. P. & HARTMANN, R. 2011. **Crystal structure of Zebrafish interferons I and II reveals conservation of type I interferon structure in vertebrates.** *J Virol,* 85**,** 8181-7.

HAUGLAND, G. T., IMSLAND, A. K., REYNOLD, P. & TREASURER, J. 2020. 10 - **Application of biological control: use of cleaner fish**. *Aquaculture Health Management* 319-369.

HAUGLAND, G. T., JAKOBSEN, R. A., VESTVIK, N., ULVEN, K., STOKKA, L. & WERGELAND, H. I. 2012. **Phagocytosis and Respiratory Burst Activity in Lumpsucker (*Cyclopterus lumpus* L.) Leucocytes Analysed by Flow Cytometry.** *Plos One,* 7.

HAUGLAND, G. T., RØNNESETH, A. & WERGELAND, H. I. 2018. **Immunology and vaccinology of lumpfish and wrasse**. *In:* TREASURER, J. (ed.) *Cleaner fish biology and aquaculture applications.* 5M Publishing Ltd.

HIRONO, I., TAKAMI, M., MIYATA, M., MIYAZAKI, T., HAN, H. J., TAKANO, T., ENDO, M. & AOKI, T. 2004. **Characterization of gene structure and expression of two toll-like receptors from Japanese flounder, *Paralichthys olivaceus***. *Immunogenetics,* 56**,** 38-46.

HU, Y., YOSHIKAWA, T., CHUNG, S., HIRONO, I. & KONDO, H. 2017. **Identification of 2 novel type I IFN genes in Japanese flounder, *Paralichthys olivaceus***. *Fish Shellfish Immunol,* 67**,** 7-10.

HUANG, B., WANG, Z. X., LIANG, Y., ZHAI, S. W., HUANG, W. S. & NIE, P. 2019. **Identification of four type I IFNs from Japanese eel with differential expression properties and Mx promoter inducibility**. *Dev Comp Immunol,* 91**,** 62-71.

HUANG, Z., CHEN, S., LIU, J., XIAO, J., YAN, J. & FENG, H. 2015. **IFNa of black carp is an antiviral cytokine modified with N-linked glycosylation**. *Fish Shellfish Immunol,* 46**,** 477-85.

JEANNIN, P., JAILLON, S. & DELNESTE, Y. 2008. **Pattern recognition receptors in the immune response against dying cells**. *Curr Opin Immunol,* 20**,** 530-7.

JENSEN, E. M., HORSBERG, T. E., SEVATDAL, S. & HELGESEN, K. O. 2020. **Trends in de-lousing of Norwegian farmed salmon from 2000-2019-Consumption of medicines, salmon louse resistance and non-medicinal control methods**. *Plos One,* 15.

JIN, M. S. & LEE, J. O. 2008. **Structures of the toll-like receptor family and its ligand complexes**. *Immunity,* 29**,** 182-91.

JOHANSEN, R. & NYLUND, S. 2021. **Rogkjeks helsestatus 2020 med vekt på Flavivirus** *Fiskehelserapport-møte*

KHOW, O. & SUNTRARACHUN, S. 2012. **Strategies for production of active eukaryotic proteins in bacterial expression system**. *Asian Pac J Trop Biomed,* 2**,** 159-62.

KILENG, O., ALBUQUERQUE, A. & ROBERTSEN, B. 2008. **Induction of interferon system genes in Atlantic salmon by the imidazoquinoline S-27609, a ligand for Toll-like receptor 7**. *Fish Shellfish Immunol,* 24**,** 514-22.

KITAO, Y., KONO, T., KORENAGA, H., IIZASA, T., NAKAMURA, K., SAVAN, R. & SAKAI, M. 2009. **Characterization and expression analysis of type I interferon in common carp Cyprinus carpio L**. *Mol Immunol,* 46**,** 2548-56.

KONGCHUM, P., HALLERMAN, E. M., HULATA, G., DAVID, L. & PALTI, Y. 2011. **Molecular cloning, characterization and expression analysis of TLR9, MyD88 and TRAF6 genes in common carp (*Cyprinus carpio*)**. *Fish Shellfish Immunol,* 30**,** 361-71.

LAGHARI, Z. A., CHEN, S. N., LI, L., HUANG, B., GAN, Z., ZHOU, Y., HUO, H. J., HOU, J. & NIE, P. 2018. **Functional, signalling and transcriptional differences of three distinct type I IFNs in a perciform fish, the mandarin fish *Siniperca chuatsi***. *Dev Comp Immunol,* 84**,** 94-108.

LAING, K. J., PURCELL, M. K., WINTON, J. R. & HANSEN, J. D. 2008. **A genomic view of the NOD-like receptor family in teleost fish: identification of a novel NLR subfamily in zebrafish**. *BMC Evol Biol,* 8**,** 42.

LARSEN, K. 2019. **Pasteurella sp. hos rognkjeks (*cyclopterus lumpus*) - antibakteriell behandling of medfødte immunresponser**. University of Bergen

LAZARTE, J. M. S., THOMPSON, K. D. & JUNG, T. S. 2019. **Pattern Recognition by Melanoma Differentiation-Associated Gene 5 (Mda5) in Teleost Fish: A Review**. *Frontiers in Immunology,* 10.

LI, Y., LI, Y., CAO, X., JIN, X. & JIN, T. 2017. **Pattern recognition receptors in zebrafish provide functional and evolutionary insight into innate immune signaling pathways**. *Cell Mol Immunol,* 14**,** 80-89.

LIAO, Z., WAN, Q. & SU, J. 2016. **Bioinformatical analysis of organizational and expressional characterizations of the IFNs, IRFs and CRFBS in grass carp, *Ctenopharygodon idella.*** *Dev comp immunol,* 61, 97-106

LIANG, B. & SU, J. 2021. **Advances in aquatic RIG-I-like receptors** *Fish and Shellfish Immunology Reports*

LIU, F., BOLS, N. C., PHAM, P. H., SECOMBES, C. J. & ZOU, J. 2019. **Evolution of IFN subgroups in bony fish - 1:Group I-III IFN exist in early ray-finned fish, with group II IFN subgroups present in the Holostean spotted gar, *Lepisosteus oculatus***. *Fish Shellfish Immunol,* 95**,** 163-170.

LIU, F., WANG, T., PETIT, J., FORLENZA, M., CHEN, X., CHEN, L., ZOU, J. & SECOMBES, C. J. 2020. **Evolution of IFN subgroups in bony fish - 2. analysis of subgroup appearance and expansion in teleost fish with a focus on salmonids**. *Fish Shellfish Immunol,* 98**,** 564-573.

LUNDE, H. S., EGGESTØL, H. O. & HAUGLAND, G. T. 2019. **TLRs and TLR signaling in lumpfish (*Cyclopterus lumpus* L.)**. *EAFP conference.* Porto, Portugal

LV, J., HUANG, R., LI, H., LUO, D., LIAO, L., ZHU, Z. & WANG, Y. 2012. **Cloning and characterization of the grass carp (*Ctenopharyngodon idella*) Toll-like receptor 22 gene, a fish-specific gene**. *Fish Shellfish Immunol,* 32**,** 1022-31.

MAEKAWA, S., AOKI, T. & WANG, H. C. 2017. **Constitutive overexpressed type I interferon induced downregulation of antiviral activity in medaka fish (*Oryzias latipes*).** *Dev Comp Immunol,* 68**,** 12-20.

MATSUSHIMA, N., TANAKA, T., ENKHBAYAR, P., MIKAMI, T., TAGA, M., YAMADA, K. & KUROKI, Y. 2007. **Comparative sequence analysis of leucine-rich repeats (LRRs) within vertebrate toll-like receptors**. *BMC Genomics,* 8**,** 124.

MILNE, D. J., CAMPOVERDE, C., ANDREE, K. B., CHEN, X., ZOU, J. & SECOMBES, C. J. 2018. **The discovery and comparative expression analysis of three distinct type I interferons in the perciform fish, meagre (*Argyrosomus regius*)**. *Dev Comp Immunol,* 84**,** 123-132.

MULLER, P. Y., JANOVJAK, H., MISEREZ, A. R. & DOBBIE, Z. 2002. **Processing of gene expression data generated by quantitative real-time RT-PCR**. *Biotechniques,* 32**,** 1372-4, 1376, 1378-9.

NERBØVIK, I. G., SOLHEIM, M. A., EGGESTØL, H. O., RØNNESETH, A., JAKOBSEN, R. A., WERGELAND, H. I. & HAUGLAND, G. T. 2017. **Molecular cloning of MDA5, phylogenetic analysis of RIG-I-like receptors (RLRs) and differential gene**

expression of RLRs, interferons and proinflammatory cytokines after in vitro challenge with IPNV, ISAV and SAV in the salmonid cell line TO. *J Fish Dis,* 40**,** 1529-1544.

NORWEGIAN DIRECTORY OF FISHERIES. (2021). **Sale of farmed cleanerfish 2012-2020.** Available from: https://www.fiskeridir.no/English/Aquaculture/Statistics/Cleanerfish-Lumpfish-and-Wrasse

O'NEILL, L. A. & BOWIE, A. G. 2007. **The family of five: TIR-domain-containing adaptors in Toll-like receptor signalling**. *Nat Rev Immunol,* 7**,** 353-64.

ONOMOTO, K., ONOGUCHI, K. & YONEYAMA, M. 2021. **Regulation of RIG-I-like receptor-mediated signaling: interaction between host and viral factors**. *Cell Mol Immunol,* 18**,** 539-555.

OVERTON, K., BARRETT, L. T., OPPEDAL, F., KRISTIANSEN, T. S. & DEMPSTER, T. 2020. **Sea lice removal by cleaner fish in salmon aquaculture: a review of the evidence base**. *Aquaculture Environment Interactions,* 12**,** 31-44.

PALTI, Y. 2011. **Toll-like receptors in bony fish: from genomics to function**. *Dev Comp Immunol,* 35**,** 1263-72.

PARK, J. H., KIM, Y. G., MCDONALD, C., KANNEGANTI, T. D., HASEGAWA, M., BODY-MALAPEL, M., INOHARA, N. & NUNEZ, G. 2007. **RICK/RIP2 mediates innate immune responses induced through Nod1 and Nod2 but not TLRs**. *Journal of Immunology,* 178**,** 2380-2386.

PEREIRO, P., COSTA, M. M., DIAZ-ROSALES, P., DIOS, S., FIGUERAS, A. & NOVOA, B. 2014. **The first characterization of two type I interferons in turbot (*Scophthalmus maximus*) reveals their differential role, expression pattern and gene induction**. *Dev Comp Immunol,* 45**,** 233-44.

PONTIGO, J. P., AGUERO, M. J., SANCHEZ, P., OYARZUN, R., VARGAS-LAGOS, C., MANCILLA, J., KOSSMANN, H., MORERA, F. J., YANEZ, A. J. & VARGAS-CHACOFF, L. 2016. **Identification and expressional analysis of NLRC5**

inflammasome gene in smolting Atlantic salmon (*Salmo salar*). *Fish & Shellfish Immunology,* 58**,** 259-265.

POWELL, A., TREASURER, J. W., POOLEY, C. L., KEAY, A. J., LLOYD, R., IMSLAND, A. K. & DE LEANIZ, C. G. 2018. **Use of lumpfish for sea-lice control in salmon farming: challenges and opportunities**. *Reviews in Aquaculture,* 10**,** 683-702.

RAJENDRAN, K. V., ZHANG, J. R., LIU, S. K., PEATMAN, E., KUCUKTAS, H., WANG, X. L., LIU, H., WOOD, T., TERHUNE, J. & LIU, Z. J. 2012. **Pathogen recognition receptors in channel catfish: II. Identification, phylogeny and expression of retinoic acid-inducible gene I (RIG-I)-like receptors (RLRs)**. *Developmental and Comparative Immunology,* 37**,** 381-389.

RANJAN, P., BOWZARD, J. B., SCHWERZMANN, J. W., JEISY-SCOTT, V., FUJITA, T. & SAMBHARA, S. 2009. **Cytoplasmic nucleic acid sensors in antiviral immunity**. *Trends Mol Med,* 15**,** 359-68.

ROBERTSEN, B. 2018. **The role of type I interferons in innate and adaptive immunity against viruses in Atlantic salmon**. *Dev Comp Immunol,* 80**,** 41-52.

ROBERTSEN, B., BERGAN, V., ROKENES, T., LARSEN, R. & ALBUQUERQUE, A. 2003. **Atlantic salmon interferon genes: cloning, sequence analysis, expression, and biological activity**. *J Interferon Cytokine Res,* 23**,** 601-12.

RØNNESETH, A., GHEBRETNSAE, D. B., WERGELAND, H. I. & HAUGLAND, G. T. 2015. **Functional characterization of IgM+ B cells and adaptive immunity in lumpfish (*Cyclopterus lumpus* L.).** *Dev Comp Immunol,* 52**,** 132-43.

SABBAH, A., CHANG, T. H., HARNACK, R., FROHLICH, V., TOMINAGA, K., DUBE, P. H., XIANG, Y. & BOSE, S. 2009. **Activation of innate immune antiviral responses by Nod2**. *Nat Immunol,* 10**,** 1073-80.

SADLER, A. J. & WILLIAMS, B. R. 2008. **Interferon-inducible antiviral effectors**. *Nat Rev Immunol,* 8**,** 559-68.

SALINAS, I. 2015. **The Mucosal Immune System of Teleost Fish**. *Biology (Basel),* 4**,** 525-39.

SCHOLZ, F., GLOSVIK, H. & MARCOS-LOPEZ, M. 2018. **Cleaner fish health**. *In:* TREASURER, J. (ed.) *Cleaner fish biology and aquaculture applications*

SHEPARD, H. M., LEUNG, D., STEBBING, N. & GOEDDEL, D. V. 1981. **A single amino acid change in IFN-beta1 abolishes its antiviral activity**. *Nature,* 294**,** 563-5.

SKOGE, R. H., BRATTESPE, J., OKLAND, A. L., PLARRE, H. & NYLUND, A. 2018. **New virus of the family Flaviviridae detected in lumpfish (*Cyclopterus lumpus*).** *Arch Virol,* 163**,** 679-685.

SRIVASTAVA, P., BHATTACHARAYA, P., PANDEY, G. & MUKHERJEE, K. J. 2005. **Overexpression and purification of recombinant human interferon alpha2b in *Escherichia coli***. *Protein Expr Purif,* 41**,** 313-22.

STAFFORD, J. L., ELLESTAD, K. K., MAGOR, K. E., BELOSEVIC, M. & MAGOR, B. G. 2003. **A toll-like receptor (TLR) gene that is up-regulated in activated goldfish macrophages**. *Developmental and Comparative Immunology,* 27**,** 685-698.

STAGG, H. E. B., GUDMUNDSDOTTIR, S., VENDRAMIN, N., RUANE, N. M., SIGURDARDOTTIR, H., CHRISTIANSEN, D. H., CUENCA, A., PETERSEN, P. E., MUNRO, E. S., POBOV, V. L., SUBRAMANIAM, K., IMNOI, K., WALTZEK, T. B. & OLESEN, N. J. 2020. **Characterization of ranaviruses isolated from lumpfish Cyclopterus lumpus L. in the North Atlantic area: proposal for a new ranavirus species (European North Atlantic Ranavirus)**. *Journal of General Virology,* 101**,** 198-207.

STEIN, C., CACCAMO, M., LAIRD, G. & LEPTIN, M. 2007. **Conservation and divergence of gene families encoding components of innate immune response systems in zebrafish.** *Genome Biol,* 8**,** R251.

STUDER, G., REMPFER, C., WATERHOUSE, A. M., GUMIENNY, R., HAAS, J. & SCHWEDE, T. 2020. **QMEANDisCo-distance constraints applied on model quality estimation**. *Bioinformatics,* 36**,** 2647.

STUDER, G., TAURIELLO, G., BIENERT, S., BIASINI, M., JOHNER, N. & SCHWEDE, T. 2021. **ProMod3-A versatile homology modelling toolbox**. *PLoS Comput Biol,* 17**,** e1008667.

SVINGERUD, T., SOLSTAD, T., SUN, B., NYRUD, M. L., KILENG, O., GREINER-TOLLERSRUD, L. & ROBERTSEN, B. 2012. **Atlantic salmon type I IFN subtypes show differences in antiviral activity and cell-dependent expression: evidence for high IFNb/IFNc-producing cells in fish lymphoid tissues**. *J Immunol,* 189**,** 5912-23.

TAKANO, T., HWANG, S. D., KONDO, H., HIRONO, I., AOKI, T. & SANO, M. 2010. **Evidence of Molecular Toll-like Receptor Mechanisms in Teleosts**. *Fish Pathology,* 45**,** 1-16.

TSUJITA, T., TSUKADA, H., NAKAO, M., OSHIUMI, H., MATSUMOTO, M. & SEYA, T. 2004. **Sensing bacterial flagellin by membrane and soluble orthologs of Toll-like receptor 5 in rainbow trout (*Onchorhynchus mykiss*).** *J Biol Chem,* 279**,** 48588-97.

VALERO, Y., MORCILLO, P., MESEGUER, J., BUONOCORE, F., ESTEBAN, M. A., CHAVES-POZO, E. & CUESTA, A. 2015. **Characterization of the IFN pathway in the teleost fish gonad against vertically transmitted viral nervous necrosis virus**. *J Gen Virol,* 96**,** 2176-2187.

VERHELST, J., HULPIAU, P. & SAELENS, X. 2013. **Mx proteins: antiviral gatekeepers that restrain the uninvited**. *Microbiol Mol Biol Rev,* 77**,** 551-66.

WAN, Q., WICRAMAARACHCHI, W. D., WHANG, I., LIM, B. S., OH, M. J., JUNG, S. J., KIM, H. C., YEO, S. Y. & LEE, J. 2012. **Molecular cloning and functional characterization of two duplicated two-cysteine containing type I interferon genes in rock bream *Oplegnathus fasciatus***. *Fish Shellfish Immunol,* 33**,** 886-98.

WANG, Y., LI, J., HAN, J., SHU, C. & XU, T. 2016. **Identification and characteristic analysis of TLR28: A novel member of the TLR1 family in teleost**. *Dev Comp Immunol,* 62**,** 102-7.

WATERHOUSE, A., BERTONI, M., BIENERT, S., STUDER, G., TAURIELLO, G., GUMIENNY, R., HEER, F. T., DE BEER, T. A. P., REMPFER, C., BORDOLI, L., LEPORE, R. & SCHWEDE, T. 2018. **SWISS-MODEL: homology modelling of protein structures and complexes**. *Nucleic Acids Res,* 46**,** W296-W303.

WORKENHE, S. T., RISE, M. L., KIBENGE, M. J. & KIBENGE, F. S. 2010. **The fight between the teleost fish immune response and aquatic viruses**. *Mol Immunol,* 47**,** 2525-36.

WU, H., LIU, L., WU, S., WANG, C., FENG, C., XIAO, J. & FENG, H. 2018. **IFNb of black carp functions importantly in host innate immune response as an antiviral cytokine**. *Fish Shellfish Immunol,* 74**,** 1-9.

XIE, J., HODGKINSON, J. W., KATZENBACK, B. A., KOVACEVIC, N. & BELOSEVIC, M. 2013. **Characterization of three Nod-like receptors and their role in antimicrobial responses of goldfish (*Carassius auratus* L.) macrophages to Aeromonas salmonicida and Mycobacterium marinum**. *Dev Comp Immunol,* 39**,** 180-7.

YU, M. & LEVINE, S. J. 2011. **Toll-like receptor 3, RIG-I-like receptors and the NLRP3 inflammasome: Key modulators of innate immune responses to double-stranded RNA viruses.** *Cytokine & Growth Factor Reviews,* 22**,** 63-72.

ZHANG, L., GAO, Z., YU, L., ZHANG, B., WANG, J. & ZHOU, J. 2018. **Nucleotide-binding and oligomerization domain (NOD)-like receptors in teleost fish: Current knowledge and future perspectives**. *J Fish Dis,* 41**,** 1317-1330.

ZHANG, Y. B. & GUI, J. F. 2012. **Molecular regulation of interferon antiviral response in fish**. *Dev Comp Immunol,* 38**,** 193-202.

ZHOU, Z., LIN, Z., PANG, X., SHAN, P. & WANG, J. 2018. **MicroRNA regulation of Toll-like receptor signaling pathways in teleost fish**. *Fish Shellfish Immunol,* 75**,** 32-40.

ZHOU, Z. X., ZHANG, B. C. & SUN, L. 2014. **Poly(I:C) induces antiviral immune responses in Japanese flounder (*Paralichthys olivaceus*) that require TLR3 and MDA5 and is negatively regulated by Myd88**. *PLoS One,* 9**,** e112918.

ZHU, L. Y., NIE, L., ZHU, G., XIANG, L. X. & SHAO, J. Z. 2013. **Advances in research of fish immune-relevant genes: A comparative overview of innate and adaptive immunity in teleosts**. *Developmental and Comparative Immunology,* 39**,** 39-62.

ZOU, J., CHANG, M., NIE, P. & SECOMBES, C. J. 2009. **Origin and evolution of the RIG-I like RNA helicase gene family**. *BMC Evol Biol,* 9**,** 85.

ZOU, J., GORGOGLIONE, B., TAYLOR, N., SUMMATHED, T., LEE, P.-T., PANIGRAHI, A., GENET, C., CHEN, Y.-M., CHEN, T. Y., HASSAN, M. U., MUGHAL, S., BOUDINOT, P. & SECOMBES, C. J. 2021. **Salmonides Have an Extraordinary Complex Type I IFN system: Characterization of the IFN locus in Rainbow Trout *Oncorhynchus mykiss* Reveals Two Novel IFN subgroups** *The journal of Immunology*.

ZOU, J. & SECOMBES, C. J. 2011. **Teleost fish interferons and their role in immunity**. *Dev Comp Immunol,* 35**,** 1376-87.

ZOU, J., TAFALLA, C., TRUCKLE, J. & SECOMBES, C. J. 2007. **Identification of a second group of type I IFNs in fish sheds light on IFN evolution in vertebrates**. *J Immunol,* 179**,** 3859-71.

ZOU, J. C., R. TAFALLA, C. 2016. **Antiviral Immunity: origin and Evolution in Vertebrates**. *In:* MALAGOLI, D. (ed.) *The Evolution of the Immune System.*

AAEN, S. M., HELGESEN, K. O., BAKKE, M. J., KAUR, K. & HORSBERG, T. E. 2015. **Drug resistance in sea lice: a threat to salmonid aquaculture**. *Trends Parasitol,* 31**,** 72-81.

8. SUPPLEMENTARY DATA

Table 8.1 P-Values from two-way ANOVA statistical analysis (with Tukey´s honest square difference post hoc test) of IFN MNE values in nine tissues. P-values < 0.05 are considered significant and ***=p<0.001, **=p<0.01 and *=p<0.05.

Tissue	IFNh (p-values)	IFNc (p-values)	IFNd (p-values)
Back vs. Thymus	0.07	0.020	0.067
Back vs. Kidney	0.096	<0.001	0.064
Back vs. Gill	0.129	0.013	0.073
Back vs. Liver	0.131	<0.001	0.019
Back vs. Front	329	0.355	0.209
Back vs. Muscle	0.347	0.004	0.058
Back vs. Skin	0.619	1.00	0.632
Back vs. Spleen	0.716	0.020	0.612
Spleen vs. Thymus	0.924	1.00	0.937
Spleen vs. Kidney	0.956	0.830	0.932
Spleen vs. Gill	0.978	1.00	0.946
Spleen vs. Liver	0.979	0.974	0.711
Spleen vs. Front	1.00	0.924	0.998
Spleen vs. Muscle	1.00	1.00	0.921
Spleen vs. Skin	1.00	0.060	1.00
Skin vs. Thymus	0.961	0.059	0.928
Skin vs. Kidney	0.980	<0.001	0.922
Skin vs. Gill	0.991	0.041	0.938
Skin vs. Liver	0.992	0.003	0.690
Skin vs. Front	1.00	0.611	0.997
Skin vs. Muscle	1.00	0.013	0.910
Muscle vs. Thymus	0.998	1.00	1.00
Muscle vs. Kidney	0.999	0.988	1.00
Muscle vs. Gill	1.00	1.00	1.00
Muscle vs. Liver	1.00	1.00	1.00
Muscle vs. Front	1.00	0.620	1.00
Front vs. Thymus	0.998	0.923	1.00
Front vs. Kidney	1.00	0.115	1.00
Front vs. Gill	1.00	0.868	1.00
Front vs. Liver	1.00	0.297	0.983
Liver vs. Thymus	1.00	0.975	1.00
Liver vs. Kidney	1.00	1.00	1.00
Liver vs. Gill	1.00	0.990	1.00
Gill vs. Thymus	1.00	1.00	1.00
Gill vs. Kidney	1.00	0.897	1.00
Kidney vs. Thymus	1.00	0.833	1.00

Table 8.2 P-Values from two-way ANOVA statistical analysis (with Tukey´s honest square difference post hoc test) of IFN MNE value after in lumpfish HKLs were stimulated with polyI:C, R848 and V. anguillarum in vitro. P-values < 0.05 are considered significant and ***=*p<0.001, **=p<0.01 and *=p<0.05. C= Control, P = polyI:C, R=R848 and B= V. anguillarum*

	IFNh		**IFNc**		**IFNd**		**IL-1β**	
	4h	24h	4h	24h	4h	24h	4h	24h
C vs. P	<0.001	<0.001	<0.001	<0.001	0.647	0.554	0.658	0.761
C vs. R	0.007	0.002	0.155	<0.001	0.99	0.99	0.893	0.981
C vs. B	0.184	<0.001	1.00	0.007	0.016	0.980	0.148	<0.001
Normality	0.196		0.640		0.859		0.221	
24 h vs 6 h	0.061		<0,001		0.809		0.275	

Table 8.3 P-Values from two-way ANOVA statistical analysis (with Tukey´s honest square difference post hoc test) of IFN MNE value after lumpfish were injected with polyI:C *in vivo*. P-values < 0.05 are considered significant and ***=p<0.001, **=p<0.01 and *=p<0.05. C= Control, P = polyI:C

	IFNh		**IFNc**		**IFNd**	
	6h	24h	6h	24h	6h	24h
			Spleen			
C vs. P	<0.001	<0.001	<0.001	<0.001	0.195	0.022
Normality	0.327		0.917		0.939	
6 vs. 24	<0.001		<0.001		0.851	
			Head kidney			
C vs. P	<0.001	0.027	0.018	0.002		
Normality	0.098		P>0.050		P>0.050	
6. vs. 24	<0.001		0.598			